Computer Physics Communications 277 (2022) 108368

Contents lists available at ScienceDirect

Computer Physics Communications

www.elsevier.com/locate/cpc

ECCPA: Calculation of classical and quantum cross sections for elastic collisions of charged particles with atoms ☆,☆☆

Francesc Salvat [a,*], Josep Llosa [a], Antonio M. Lallena [b], Julio Almansa [c]

[a] Facultat de Física (FQA and ICC), Universitat de Barcelona, Diagonal 645, 08028 Barcelona, Catalonia, Spain
[b] Departamento de Física Atómica, Molecular y Nuclear. Universidad de Granada, E-18071 Granada, Spain
[c] Servicio de Radiofísica y P.R., Hosp. Univ. Virgen de las Nieves, Avda. de las Fuerzas Armadas 2, E-18014 Granada, Spain

ARTICLE INFO

Article history:
Received 21 October 2021
Received in revised form 18 March 2022
Accepted 1 April 2022
Available online 11 April 2022

Keywords:
Elastic collisions
Classical scattering theory
Relativistic collisions
Eikonal approximation
Born approximation
Partial-wave analysis
WKB phase shifts

ABSTRACT

The Fortran program ECCPA calculates differential and integrated cross sections for elastic collisions of charged particles with atoms by using the classical-trajectory method and several quantum methods and approximations. The collisions are described within the framework of the static-field approximation, with the interaction between the projectile and the target atom represented by the Coulomb potential of the atomic nucleus screened by the atomic electrons. To allow the use of fast and robust calculation methods, the interaction is assumed to be the same in the center-of-mass frame and in the laboratory frame. Although this assumption neglects the effect of relativity on the interaction, it allows using strict relativistic kinematics. The equation of the relative motion in the center-of-mass frame is shown to have the same form as in the non-relativistic theory, with a relativistic reduced mass and an effective potential. The wave equation for the relative motion, as obtained from the correspondence principle, is formally identical to the non-relativistic Schrödinger equation with the reduced mass and the effective potential, and it reduces to the familiar Klein-Gordon equation when the mass of the target atom is much larger than that of the projectile. Collisions of spin 1/2 projectiles are also described by solving the Dirac wave equation. Various approximate solution methods are described and applied to a generic potential represented as a sum of Yukawa terms, which allows a good part of the calculations to be performed analytically. The program ECCPA is useful for assessing the validity and the relative accuracy of the various approximations, and as a pedagogical tool.

Program summary

Program Title: ECCPA
CPC Library link to program files: https://doi.org/10.17632/c3tn9hyfvb.1
Licensing provisions: CC by NC 3.0
Programming language: Fortran 90/95
Nature of problem: The program computes differential cross sections (DCSs) for elastic collisions of charged particles (electrons, positrons, muons, antimuons, protons, antiprotons, and alphas) with neutral atoms. Calculations are performed within the static-field approximation with screened Coulomb potentials expressed as a sum of Yukawa terms with their parameters fitted to approximate the atomic electrostatic potentials resulting from the Thomas–Fermi model and from self-consistent Dirac–Hartree–Fock–Slater calculations. The program ECCPA provides DCSs computed with four different approaches: the classical trajectory method, the Born approximation, the partial-wave expansion method with approximate phase shifts, and the eikonal approximation. The user is allowed to select the atomic number of the target atom, the potential model, the kind of projectile and its kinetic energy. Calculation results are written in a number of output files with formats suited for visualization with a plotting program. A Java graphical user interface allows running the program and visualizing the results interactively.
Solution method: A relativistic extension of the classical trajectory method is formulated on the assumption that the interaction in the center-of-mass frame is central, which is a fundamental

☆ The review of this paper was arranged by Prof. Stephan Fritzsche.
☆☆ This paper and its associated computer program are available via the Computer Physics Communications homepage on ScienceDirect (http://www.sciencedirect.com/science/journal/00104655).

* Corresponding author.
E-mail address: francesc.salvat@ub.edu (F. Salvat).

https://doi.org/10.1016/j.cpc.2022.108368

requirement of the adopted calculation schemes; the DCS in the laboratory frame is then obtained from the relativistic (Lorentz) transform of the DCS calculated in the center-of-mass frame. This scheme qualifies as semi-relativistic, because it accounts for relativistic kinematics in a rigorous way, but disregards the differences between the interactions observed from the laboratory and the center-of-mass frames. We consider the elementary quantum formulation based on the relativistic Schrödinger (or Klein–Gordon) wave equation obtained from the correspondence principle. Accurate DCSs for potential scattering can be computed by using the partial-wave expansion method, at the expense of considerable numerical work. To avoid the difficult calculation of phase shifts from the numerical solution of the radial wave equation, we adopt a simplified strategy that combines the (first) Born approximation, for both the scattering amplitude and the phase shifts, and the Wentzel–Kramers–Brillouin (WKB) approximation for the phase shifts. We also describe the semi-classical eikonal approximation, which is known to yield reliable DCSs for collisions with small scattering angles. The case of collisions of electrons and positrons is considered on similar grounds, with the scattering amplitudes obtained from the Dirac equation.

The numerical work is simplified by approximating the interaction potential as a sum of Yukawa terms, which allows performing a good part of the calculations analytically. Integrals of functions given by analytical formulas are calculated by means of an adaptive algorithm that combines the 20-point Gauss-Legendre quadrature formula with a bisection scheme; this algorithm allows strict control of numerical errors and gives results with a relative accuracy better than about 10^{-10} for well-behaved integrands. The whole calculation for a given energy of the projectile takes no longer than a few seconds on a modern personal computer, quite irrespectively of the energy and of the atomic number of the target atom.

Additional comments including restrictions and unusual features: The adopted interaction potentials correspond to atoms with point nuclei. The use of a parameterization instead of numerical tables of the potential (obtained, *e.g.*, from atomic structure calculations) has a minor effect on the calculated DCSs. This effect is limited to large scattering angles, where the actual DCS does differ from calculations with screened Coulomb potentials due to the effect of the finite size and structure of the atomic nucleus, which is disregarded here.

DCSs obtained from the partial-wave expansion method and with the eikonal approximation provide a fairly accurate description of collisions with small and moderate deflection angles. They can be used, *e.g.*, in Monte Carlo simulations of the transport of fast charged particles in matter. The information generated by the program allows assessing the accuracy of calculations with the various approaches, and permits identifying the ranges of validity of the classical trajectory method and the Born approximation.

1. Introduction

Elastic collisions of charged particles with atoms play a central role in theoretical radiation physics. By definition, elastic collisions are interactions that do not cause excitation of the target atom, which usually is in its ground state. These collisions may produce large deflections of the projectile and, consequently, have a direct effect on the structure of trajectories of fast charged particles moving in material media. In addition, each collision involves an energy transfer from the projectile to the target atom which manifests as the recoil of the latter after the interaction and gives rise to the so-called *nuclear* contribution to the stopping power.

Elastic collisions are usually described by means of the theory of scattering by central potentials. The non-relativistic theory is studied in most textbooks of both classical [1,2] and quantum mechanics [3–5]. Calculations normally assume that the potential is central because this is the only case that admits practicable formal or numerical solutions. In the case of collisions with a bare point nucleus, the interaction reduces to the Coulomb potential and the problem can be solved analytically; the corresponding differential cross section (DCS) is given by the famous analytical formula derived by Rutherford [6], which was instrumental in the discovery of the atomic nucleus. The calculation of elastic collisions with neutral atoms (*i.e.*, of the scattering by screened Coulomb potentials) is more difficult, because it has to be performed numerically. The non-relativistic classical trajectory method [2] allows the calculation of the DCS through a set of quadratures [7].

In a quantum formulation, the scattering amplitude is expressed as a partial-wave series, *i.e.*, as a Legendre series with coefficients determined by the scattering phase shifts, which represent the effect of the potential on the asymptotic behavior of spherical waves with well-defined angular momentum. Numerical calculations with this scheme are feasible for electrons and positrons; the Fortran program ELSEPA [8] calculates very accurate DCSs for these particles by using the relativistic (Dirac) partial-wave method with arbitrary screened atomic potentials. Unfortunately, similar calculations for heavier projectiles are not doable because the short de Broglie wave lengths of these projectiles make the numerical solution of the radial wave equation extremely difficult; in addition, the corresponding partial-wave series converge very slowly. Consequently, one must have recourse to approximation methods.

Although the essentials of the theory of scattering by central potentials and of elastic collisions of charged particles are covered in graduate courses and textbooks, comparisons of results from different approximations are hard to find in the literature. These comparisons are important to illustrate the capabilities and limitations of the theoretical approaches. In the present article we describe several approximate methods that allow the fast calculation of DCSs for elastic collisions of charged particles with neutral atoms.

We have written a Fortran program named ECCPA that computes elastic collisions of electrons, muons, protons (and the antiparticles of the three) and alphas with atoms. This program provides the DCS (in the center-of-mass and the laboratory frames) calculated by using the following theoretical approaches:

- the method of classical trajectories,
- the first Born approximation,
- the partial-wave expansion method with phase shifts obtained from the Born and WKB approximations, and

- the eikonal approximation.

Both the partial-wave expansion method and the eikonal approximation involve a great deal of numerical work for potentials given in numerical form. To alleviate the work without sacrificing the reliability of the calculated DCSs, we consider interaction potentials expressed as a sum of Yukawa-like terms, with parameters determined by fitting realistic atomic potentials. Potentials with this analytical form allow performing a good part of the calculations analytically, and reduce the evaluation of the DCS to a set of integrals of functions of a single variable.

Although ECCPA works for projectiles with arbitrary kinetic energies, provided it does not encounter numerical conflicts, the calculated DCSs are reliable (*i.e.*, consistent with measurements) only for a limited range of kinetic energies of the projectile, which is determined by the simplifications of the underlying model. On one hand, the target atom is considered as a rigid distribution of charge, and the projectile is assumed to travel "naked" (*i.e.*, the possible capture of electrons by positively-charged projectiles is disregarded). These simplifications are valid only for projectiles with kinetic energies larger than about 2 MeV per unified mass unit. On the other hand, our approximate treatment of relativistic effects is expected to be valid only for projectiles with kinetic energy less than about their rest energy.

Combined with a plotting program to visualize the results, ECCPA becomes a useful tool for assessing the validity of the classical trajectory method and the quantum approximations, and also for illustrating fundamental aspects of the theory. As a matter of fact, ECCPA provides all the information on elastic collisions that is needed for Monte Carlo simulation of the transport of charged particles in matter [9,10], where the evolution of individual particles is described as a sequence of random interaction events sampled from the adopted DCSs.

The present article is organized as follows. The adopted analytical forms of the atomic potentials are described in Section 2. In Section 3 we derive the relativistic equation of motion in the center-of-mass (CM) frame and we describe the calculation of the DCS by the method of classical trajectories. Section 4 deals with the relativistic wave equation for the relative motion of the colliding particles and with several methods and approximations for computing the DCS in the CM frame. The transformation of the DCS from the CM frame to the laboratory frame, where the target atom is initially at rest, is considered in Section 5. Section 6 deals with collisions of electrons and positrons, which are described on the basis of the Dirac wave equation with the aid of the Born and WKB approximations. The Fortran program ECCPA and its Java graphical interface are described in Section 7. Finally, Section 8 presents example results.

2. Interaction potential

We consider the collisions of charged particles with atoms from the standpoint of the *static-field approximation*, *i.e.*, as scattering of the projectile by the electrostatic field of the target atom, suitably averaged over directions [11,12]. It should be mentioned that this approximation gives results in good agreement with measurements only for particles with sufficiently high energies, higher than about 1 keV in the case of electrons and positrons, $\gtrsim 2$ MeV for protons. The static-field approximation disregards the effect of the dipole polarizability of the target atom, that is, the fact that the electric field of the projectile shifts the atomic charges and the induced dipole moment acts back on the projectile. This polarizability effect is appreciable only for slow projectiles and at small scattering angles (corresponding to large impact parameters), because atomic polarization is effective only under slowly-varying electric fields. In addition, results from measurements of elastic collisions are affected by inelastic interactions, which remove projectiles from the "elastic channel". Finally, in the case of projectile electrons, elastic collisions are altered by exchange effects, which result from the indistinguishability of the projectile and the electrons in the target atom. In the so-called *optical-potential models* the effects of polarization and inelastic absorption, and exchange in the case of electrons, are described approximately by means of effective local potentials with an absorptive imaginary part (see, *e.g.*, Ref. [13] and references therein).

We assume a neutral target atom of atomic number Z, with a point nucleus of charge Ze (e denotes the elementary charge) at the origin of coordinates, and a spherically symmetric cloud of Z electrons in its ground state. The interaction potential energy between the projectile (of charge $Z_1 e$) at $\mathbf{r}$ and the target atom is

$$V(r) = Z_1 e\, \varphi_{\rm es}(r)\,, \tag{1}$$

where $\varphi_{\rm es}(r)$ is the electrostatic potential of the atomic charge distribution,

$$\varphi_{\rm es}(r) = \frac{Ze}{r} - e\left(\frac{1}{r}\int_0^r \rho(r')\,4\pi r'^2\,{\rm d}r' + \int_r^\infty \rho(r')\,4\pi r'\,{\rm d}r'\right), \tag{2}$$

and $\rho(r)$ is the atomic electron density. It is customary to write

$$\varphi_{\rm es}(r) = \frac{Ze}{r}\,\Phi(r), \tag{3}$$

where $\Phi(r)$, the screening function, describes the electrostatic shielding of the nuclear charge by the atomic electrons.

To facilitate calculations, we use approximate screening functions given by the following analytical expression

$$\Phi(r) = \sum_{i=1}^{3} A_i \exp(-a_i r) \tag{4}$$

with parameters determined by fitting the numerical screening functions obtained from different atomic structure calculations. The corresponding interaction potential is

$$V(r) = \frac{Z_1 Z e^2}{r}\sum_{i=1}^{3} A_i \exp(-a_i r). \tag{5}$$

Analytical potentials of this type (a sum of Yukawa-like terms) have been used by many authors in studies of particle collisions [14,15]. In the calculations described below we consider the following screening function models and sets of parameters.

- *Thomas–Fermi–Molière (TFM) screening function*

The simplest theoretical framework to obtain approximate atomic electron densities is the Thomas–Fermi model in which the electron cloud is considered as a locally homogeneous electron gas bound by the screened Coulomb field of the nucleus. This model yields a "universal" screening function, applicable to all elements, that is determined by a differential equation. Because this equation needs to be solved numerically [16], Molière [17] used the form (4) as an approximation to the numerical Thomas–Fermi screening function with the set of parameters

$$A_1 = 0.10, \quad A_2 = 0.55, \quad A_3 = 0.35,$$
$$a_1 = 6.0/b, \quad a_2 = 1.2/b, \quad a_3 = 0.3/b, \tag{6}$$

where

$$b \equiv \frac{(3\pi)^{2/3}}{2^{7/3}} \frac{\hbar^2}{\mathrm{m_e} e^2} Z^{-1/3} = 0.88534 Z^{-1/3} a_0 \tag{7}$$

is a radial scale parameter known as the Thomas–Fermi radius, and $a_0 = \hbar^2/(\mathrm{m_e} e^2)$ is the Bohr radius, $\hbar$ is the reduced Planck constant. The approximation (6) agrees closely with the Thomas–Fermi screening function in the region $r \lesssim 6b$ where the latter takes appreciable values.

- *Dirac–Hartree–Fock–Slater (DHFS) screening function*

In general, screening functions obtained from self-consistent atomic electron densities are given numerically. In the present calculations we use the analytical approximation (4) with the set of parameters given by Salvat et al. [18], which were obtained by fitting the Dirac–Hartree–Fock–Slater self-consistent electron densities of neutral atoms [19,20]. With these parameters, the analytical approximation and the numerical DHFS potential yield the same DCSs for scattering of charged particles at small angles when calculated within the Born approximation [18], which is expected to be accurate for projectiles with sufficiently high energies (see Section 4.2).

- *The Wentzel potential*

In an early calculation of elastic scattering with the Born approximation, Wentzel [21] used a potential of the generic form (5) with the one-term screening function $\Phi_{\mathrm{W}}(r) = \exp(-ar)$,

$$V_{\mathrm{W}}(r) = \frac{Z_1 Z e^2}{r} \exp(-ar), \qquad a = 1/R, \tag{8}$$

where R is the "atomic radius" or "screening length", which is frequently approximated as

$$R = 0.88534 Z^{-1/3} a_0, \tag{9}$$

to comply with the Thomas–Fermi scaling.

3. Classical elastic collisions

Let us start with the classical calculation of collisions of a projectile particle (1) (of mass M_1 and charge $Z_1 e$) and a target atom (2) of atomic number Z (and mass M_2), which interact through the potential $V(r)$. To cover the energy range of interest in radiation transport, we use relativistic kinematics. We recall that the linear momentum $\mathbf{p}$, the kinetic energy E, and the total energy W of a particle of mass M are related by

$$(cp)^2 + M^2 c^4 = (E + Mc^2)^2 = W^2. \tag{10}$$

These quantities are conveniently expressed as

$$\mathbf{p} = \beta \gamma Mc \, \hat{\mathbf{p}}, \quad E = (\gamma - 1) Mc^2, \quad \text{and} \quad W = \gamma Mc^2, \tag{11}$$

where

$$\beta = \frac{v}{c} = \left[1 + \left(\frac{Mc}{p}\right)^2\right]^{-1/2} = \frac{\sqrt{E(E + 2Mc^2)}}{E + Mc^2} \tag{12}$$

is the velocity of the particle in units of the speed of light c, and

$$\gamma = \sqrt{\frac{1}{1 - \beta^2}} = \sqrt{1 + \left(\frac{p}{Mc}\right)^2} = \frac{E + Mc^2}{Mc^2} \tag{13}$$

is its total energy in units of the rest energy Mc^2.

In practical transport studies, collisions are described in the laboratory (L) reference frame, where initially (*i.e.*, before the collision) the target atom is at rest and the projectile moves in the direction of the z axis with linear momentum $p_{1\mathrm{i}}$. Because the interaction is central, trajectories of the colliding particles lie in a plane, the scattering plane. We set the direction of the x axis so that the z-y plane coincides with the scattering plane. Then, in the L frame, the energy-momentum four-vectors of the projectile and the target before the collision are, respectively,

$$P_{1\mathrm{i}} = (W_{1\mathrm{i}}c^{-1}, 0, 0, p_{1\mathrm{i}}) \quad \text{and} \quad P_{2\mathrm{i}} = (W_{2\mathrm{i}}c^{-1}, 0, 0, 0), \tag{14}$$

where $W_{j\mathrm{i}}$ denotes the initial energy of particle j,

$$W_{1\mathrm{i}} = E_{1\mathrm{i}} + M_1c^2 \quad \text{and} \quad W_{2\mathrm{i}} = M_2c^2, \tag{15}$$

where $E_{1\mathrm{i}}$ is the kinetic energy of the incident projectile. The four-momenta of the two particles after the collision are

$$P_{1\mathrm{f}} = (W_{1\mathrm{f}}c^{-1}, 0, p_{1\mathrm{f}}\sin\theta_1, p_{1\mathrm{f}}\cos\theta_1) \tag{16a}$$

and

$$P_{2\mathrm{f}} = (W_{2\mathrm{f}}c^{-1}, 0, p_{2\mathrm{f}}\sin\theta_2, -p_{2\mathrm{f}}\cos\theta_2). \tag{16b}$$

The kinematics of elastic collisions is simpler in the center-of-mass (CM) frame, in which the total linear momentum of the colliding particles vanishes. In CM the two particles have opposite linear momenta of equal magnitude, and the collision causes only a rotation of their linear momentum vectors. In the non-relativistic formulation, the interaction in CM is the same as in the L frame, and the motion of the projectile relative to the target is that of a single particle having the reduced mass of the pair under the action of the interaction force [2].

We shall calculate the DCS in the CM frame by solving the *relativistic* equation for the relative motion, assuming a central potential in the CM frame, and we shall infer the DCS in the L frame by means of a Lorentz boost. Specifically, we consider that the interaction in CM is the same as in the L frame, that is, we disregard the transformation properties of the electromagnetic field under Lorentz transformations (see, *e.g.*, Ref. [22]). The assumption of a central potential, which is essential to render the calculations doable, is correct for non-relativistic projectiles but it becomes inconsistent for projectiles with high energies, such that the velocity of the CM frame becomes comparable to c (partly because the FitzGerald-Lorentz contraction destroys the spherical symmetry of the interaction). Our approach qualifies as semi-relativistic, because it implements strict relativistic kinematics but disregards the effects of relativity on the interaction.

We consider that the potential $V(r)$ tends to zero at large distances, so that the four-momenta of the particles before and after the interaction are completely defined by their masses and linear momenta. We use primes to designate quantities in the CM frame. The initial four-momenta of the two particles in CM are $P'_{j\mathrm{i}} = (W'_{j\mathrm{i}}c^{-1}, \mathbf{p}'_{j\mathrm{i}})$. The CM moves with respect to the L frame with constant velocity $\mathbf{v}_{\mathrm{CM}} = v_{\mathrm{CM}}\hat{\mathbf{z}}$. The transformation from the CM to the L frame is a boost in the z direction. The four-momenta $P = (Wc^{-1}, \mathbf{p})$ and $P' = (W'c^{-1}, \mathbf{p}')$ of a particle in the L and CM frames are related by

$$\begin{aligned} W &= \gamma_{\mathrm{CM}}(W' + \beta_{\mathrm{CM}}cp'_z), \\ p_z &= \gamma_{\mathrm{CM}}(p'_z + \beta_{\mathrm{CM}}W'c^{-1}), \\ p_x &= p'_x, \quad p_y = p'_y, \end{aligned} \tag{17}$$

where

$$\beta_{\mathrm{CM}} = \frac{v_{\mathrm{CM}}}{c}, \qquad \gamma_{\mathrm{CM}} = \frac{1}{\sqrt{1-\beta_{\mathrm{CM}}^2}}. \tag{18}$$

The velocity v_{CM} of the CM frame is determined by applying the transformation (17) to the total initial four-momentum in CM, $P'_{\mathrm{i}} = P'_{1\mathrm{i}} + P'_{2\mathrm{i}} = (W'_{1\mathrm{i}}c^{-1} + W'_{2\mathrm{i}}c^{-1}, \mathbf{0})$, which gives

$$p_{1\mathrm{i}} = \gamma_{\mathrm{CM}}\beta_{\mathrm{CM}}(W'_{1\mathrm{i}} + W'_{2\mathrm{i}})c^{-1}, \qquad W_{1\mathrm{i}} + W_{2\mathrm{i}} = \gamma_{\mathrm{CM}}(W'_{1\mathrm{i}} + W'_{2\mathrm{i}}). \tag{19}$$

These equations imply that

$$\beta_{\mathrm{CM}} = \frac{cp_{1\mathrm{i}}}{W_{1\mathrm{i}} + W_{2\mathrm{i}}}. \tag{20}$$

The square of the total four-momentum of the particles,

$$s^2 \equiv c^2\,(P_1 + P_2)^2 = (W_1 + W_2)^2 - c^2\,(\mathbf{p}_1 + \mathbf{p}_2)^2\,, \tag{21}$$

is a Lorentz invariant. In the CM frame, s equals the total energy of the particles, $s = W'_1 + W'_2$. Before the interaction we have

$$s^2 = (W_{1\mathrm{i}} + W_{2\mathrm{i}})^2 - c^2p_{1\mathrm{i}}^2 = (M_1c^2 + M_2c^2)^2 + 2M_2c^2E_{1\mathrm{i}}. \tag{22}$$

The equality (20) implies that

$$\gamma_{\mathrm{CM}} = \frac{W_{1\mathrm{i}} + W_{2\mathrm{i}}}{s}. \tag{23}$$

Before the collision, in the CM frame the colliding particles have opposite linear momenta

$$\mathbf{p}'_{1\mathrm{i}} = -\mathbf{p}'_{2\mathrm{i}} \equiv \mathbf{p}'_{\mathrm{i}} \tag{24}$$

with magnitude

$$p'_{\mathrm{i}} = \beta_{\mathrm{CM}}\gamma_{\mathrm{CM}} M_2 c = \frac{M_2 c^2}{s}\, p_{1\mathrm{i}}\,. \tag{25}$$

The initial total energies of the particles are given by

$$W'_{1\mathrm{i}} = \sqrt{M_1^2c^4 + p_{\mathrm{i}}'^2 c^2} \quad \text{and} \quad W'_{1\mathrm{i}} = \sqrt{M_1^2c^4 + p_{\mathrm{i}}'^2 c^2}. \tag{26}$$

After the collision, when the interaction energy has vanished, the particles move away with linear momenta of the same magnitude p'_{i} and with the same total energies, that is,

$$W'_{1\mathrm{f}} = W'_{1\mathrm{i}} \qquad \text{and} \qquad W'_{2\mathrm{f}} = W'_{2\mathrm{i}}\,. \tag{27}$$

3.1. Relative motion in the CM frame

Let us now consider the equations of motion of the colliding particles in the CM frame,

$$\dot{\mathbf{p}}'_1 = \mathbf{F} \quad \text{and} \quad \dot{\mathbf{p}}'_2 = -\mathbf{F} \tag{28}$$

where

$$\mathbf{F} = -\frac{\mathrm{d}V}{\mathrm{d}r'}\,\hat{\mathbf{r}}', \tag{29}$$

with $\mathbf{r}' = \mathbf{r}'_1 - \mathbf{r}'_2$. Dotted quantities represent time derivatives. The relative velocity, $\mathbf{v}' = \dot{\mathbf{r}}'$, is

$$\mathbf{v}' = \mathbf{v}'_1 - \mathbf{v}'_2 = \frac{c^2\mathbf{p}'_1}{W'_1} - \frac{c^2\mathbf{p}'_2}{W'_2} = \left(\frac{c^2}{W'_1} + \frac{c^2}{W'_2}\right)\mathbf{p}', \tag{30}$$

where $\mathbf{p}' = \mathbf{p}'_1$ is the linear momentum of the projectile. Hence, the equation for the relative motion reads

$$\dot{\mathbf{v}}' = \frac{\mathrm{d}}{\mathrm{d}t}\left[\left(\frac{c^2}{W'_1} + \frac{c^2}{W'_2}\right)\mathbf{p}'\right]. \tag{31}$$

By virtue of a *vis viva* theorem, the quantity

$$\mathcal{S} \equiv W'_1 + W'_2 + V(r') \tag{32}$$

is a constant of the motion. In addition, for central forces, the angular momentum $\mathbf{L}' = \mathbf{r}' \times \mathbf{p}'$ is conserved. Because

$$\mathbf{r}' \times \mathbf{v}' = \left(\frac{c^2}{W'_1} + \frac{c^2}{W'_2}\right)\mathbf{L}', \tag{33}$$

the conservation of angular momentum implies that the trajectories of the particles lie in the plane of scattering. The values of the constants L' and $\mathcal{S}$ are determined by the initial conditions; $L' = bp'_{\mathrm{i}}$, where b is the impact parameter (which takes the same values in L and CM), and $\mathcal{S} = s$ is given by Eq. (22). With the aid of these constants of motion, the deflection angle of a projectile with a given impact parameter can be obtained by quadrature, in strict analogy with the classical non-relativistic formulation [2].

The equality

$$\mathcal{S} - V(r') = \sqrt{M_1^2c^4 + p'^2c^2} + \sqrt{M_2^2c^4 + p'^2c^2} \tag{34}$$

implies that

$$p'^2(r') = \frac{1}{4c^2}\left\{\left[\mathcal{S} - V(r')\right]^2 + \frac{\left(M_1^2 - M_2^2\right)^2 c^8}{\left[\mathcal{S} - V(r')\right]^2}\right\} - \frac{(M_1^2 + M_2^2)c^2}{2}\,. \tag{35}$$

With some rearrangements, this expression can be reduced to the familiar non-relativistic form of the equation of motion

$$p'^2(r') = p_{\mathrm{i}}'^2 - 2\mu_{\mathrm{r}} V_{\mathrm{ef}}(r') \tag{36}$$

where

$$\mu_{\mathrm{r}} = c^{-2}\,\frac{W'_{1\mathrm{i}} W'_{2\mathrm{i}}}{W'_{1\mathrm{i}} + W'_{2\mathrm{i}}}\,, \tag{37}$$

is the relativistic reduced mass of the colliding particles and $V_{\mathrm{ef}}(r')$ is an effective potential given by

$$V_{\rm ef}(r') = V(r') + V_{\rm r1}(r') + V_{\rm r2}(r'), \tag{38}$$

with

$$V_{\rm r1}(r') = -\frac{V^2(r')}{2\mu_{\rm r}c^2}\left(1 - \frac{3\mu_{\rm r}c^2}{\mathcal{S}}\right) \tag{39a}$$

and

$$V_{\rm r2}(r') = \frac{(M_1^2 - M_2^2)^2 c^6}{8\mu_{\rm r}\mathcal{S}^2}\left(\left[1 - \frac{V(r')}{\mathcal{S}}\right]^{-2} - 1 - 2\frac{V(r')}{\mathcal{S}} - 3\frac{V^2(r')}{\mathcal{S}^2}\right). \tag{39b}$$

The terms $V_{\rm r1}(r')$ and $V_{\rm r2}(r')$ are corrections to the interaction potential that account for the effect of relativistic kinematics. The first one is proportional to $V^2(r')$; when $V(r')$ is a screened Coulomb potential, $V_{\rm r1}(r')$ diverges as r'^{-2} at the origin. Considering the Taylor expansion of the function $(1-x)^{-2}$, the second correction term, $V_{\rm r2}(r)$, is seen to be of order $(V/\mathcal{S})^3$, and it vanishes when the projectile and the target particles have the same mass.

It is worth observing that when the mass M_2 of the target tends to infinity, $\beta_{\rm CM} = 0$ and the CM frame coincides with the L frame. Under these circumstances, $\mathbf{p}'_{\rm i} = \mathbf{p}_{\rm 1i}$, $s \simeq \infty$, and

$$\mu_{\rm r} \simeq \mathcal{W}_1 c^{-2} = \gamma_{\rm 1i} M_1. \tag{40}$$

That is, the reduced mass equals the relativistic mass of the projectile, which increases with $p_{\rm 1i}$.

3.2. Classical DCS in the CM frame

Since Eq. (36) has the same form as the corresponding non-relativistic equation, the calculation of the DCS can be performed by following the same steps as in the classical non-relativistic theory (see, *e.g.*, Ref. [2]). The deflection angle (*i.e.*, the total angle swept by the vector $\mathbf{p}'$) is a function of the impact parameter b, or of the angular momentum $L' = p'b$. It can be calculated as

$$\vartheta'(L') = \pi - 2\int_{r'_0}^{\infty} \frac{L' r'^{-2}}{\sqrt{p'^2_{\rm i} - 2\mu_{\rm r}V_{\rm ef}(r') - L'^2 r'^{-2}}}\,{\rm d}r', \tag{41}$$

where r'_0 is the distance of closest approach, that is, the largest root of the equation

$$p'^2_{\rm i} - 2\mu_{\rm r}V_{\rm ef}(r'_0) - \frac{L'^2}{r'^2_0} = 0\,. \tag{42}$$

It is worth recalling that if $V_{\rm ef}(r)$ is the Coulomb potential

$$V_{\rm C}(r) = \frac{Z_1 Z e^2}{r} \tag{43}$$

the deflection angle is given by [2]

$$\vartheta'_{\rm C}(L') = \pi - 2\int_{r'_0}^{\infty} \frac{L' r'^{-1}}{\sqrt{r'^2 p'^2_i - 2\mu_{\rm r}Z_1 Z e^2 r' - L'^2}}\,{\rm d}r' = 2\arctan\left(\frac{\mu_{\rm r}Z_1 Z e^2}{L' p'_{\rm i}}\right). \tag{44}$$

The numerical calculation of the angular deflection for the screened Coulomb potential (5) faces the same difficulties as in the non-relativistic case [23], namely, the divergence of the integrand at the distance of closest approach and, in the case of relatively large angular momenta, the near cancellation of the two terms on the right-hand side of Eq. (41). It is expedient to introduce the function

$$\Psi(r') = \frac{r' V_{\rm ef}(r')}{Z_1 Z e^2} \tag{45}$$

which plays a role similar to the screening function. Subtracting and adding, respectively, the second and third quantities in the equalities (44) after replacing Z with $Z\Psi(r'_0)$, and changing the integration variable to $u = (1 - r'_0/r')^{1/2}$, we have

$$\vartheta'(L') = 2\arctan\left(\frac{M Z_1 Z e^2 \Psi(r'_0)}{L' p'_{\rm i}}\right) + 4\int_0^1 \left\{\frac{1}{\sqrt{C\Psi(r'_0) + 2 - u^2}} - \frac{1}{\sqrt{C\Psi(r'_0) + 2 - u^2 - Cf(u)}}\right\}{\rm d}u\,, \tag{46}$$

where

$$C = \frac{2\mu_{\rm r}Z_1 Z e^2 r'_0}{L'^2}\,, \tag{47}$$

and

$$f(u) = r'_0 \frac{\Psi(r') - \Psi(r'_0)}{r' - r'_0} \,. \tag{48}$$

The function $f(u)$ is approximately constant for $u < 0.001$, which corresponds to radii between r'_0 and $r'_1 = (1 + 10^{-6})r'_0$, where $f(u) \simeq r'_0[\mathrm{d}\Psi(r'_0)/\mathrm{d}r'_0]$. For radii larger than r'_1, $f(u)$ can be calculated directly from the expression (48). Thus, the integrand in Eq. (46) is finite and varies smoothly over the integration interval, and the integral can be calculated numerically.

While the deflection angle ϑ' may take arbitrarily large positive or negative values, the polar scattering angle θ' is, by definition, limited to the interval $[0, \pi]$. The two angles are related by

$$\cos\theta' = \cos\vartheta' . \tag{49}$$

If the function $L'(\theta')$ is single-valued, the classical DCS in CM is

$$\frac{\mathrm{d}\sigma'}{\mathrm{d}\Omega'} = \frac{2\pi\, b\, \mathrm{d}b}{\mathrm{d}\Omega'} = \frac{1}{2\sin\theta'} \left|\frac{\mathrm{d}b^2}{\mathrm{d}\theta'}\right| = \frac{1}{2p'^2_\mathrm{i}\sin\theta'} \left|\frac{\mathrm{d}L'^2}{\mathrm{d}\theta'}\right| . \tag{50}$$

When the function $L'(\theta')$ is multi-valued, the DCS is the sum of contributions from the various branches of that function,

$$\frac{\mathrm{d}\sigma'}{\mathrm{d}\Omega'} = \frac{1}{2p'^2_\mathrm{i}\sin\theta'} \sum_j \left|\frac{\mathrm{d}L'^2}{\mathrm{d}\theta'}\right|_{L'=L'_j} , \tag{51}$$

where the summation extends over the values L'_j of the angular momentum that give deflection angles corresponding to the scattering angle θ'. In the case of the unscreened Coulomb potential, with the deflection function (44), the DCS is given by the Rutherford formula

$$\frac{\mathrm{d}\sigma'_\mathrm{Ruth}}{\mathrm{d}\Omega'} = \left(\frac{\mu_\mathrm{r} Z_1 Z e^2}{2p'^2_\mathrm{i}}\right)^2 \frac{1}{\sin^4(\theta'/2)} . \tag{52}$$

Bohr [24] used qualitative diffraction arguments to analyze the validity of the classical trajectory method. Assuming that the function $L'(\theta')$ is singly-valued, his reasoning leads to the conclusion that the classical method is valid (*i.e.*, it yields the same DCS as a quantum calculation) when

$$T_\mathrm{class}(\theta) = \frac{1}{\theta'}\sqrt{\hbar\left|\frac{\mathrm{d}\theta'}{\mathrm{d}L'}\right|} \ll 1. \tag{53}$$

In the case of a Coulomb potential, this condition implies that the classical method is valid for all angles if the absolute value of the Sommerfeld parameter

$$\eta \equiv \frac{\mu_\mathrm{r} Z_1 Z e^2}{\hbar p'_\mathrm{i}} \tag{54}$$

is much larger than unity. In the case of screened Coulomb fields, Bohr's criterion is satisfied for scattering angles larger than about

$$\theta'_\mathrm{clas} = \frac{\hbar}{p'_\mathrm{i} R} , \tag{55}$$

where R is the atomic radius, Eq. (9). When the classical method is valid, we may associate each impact parameter (or angular momentum) to a well defined scattering angle. Generally, small angles correspond to large impact parameters.

The relativistic corrections (39) to the potential $V(r)$, Eq. (38), are appreciable only for small radii, at which the actual interaction potential departs from the screened Coulomb potential due to the finite size of the nucleus. These correction terms have an influence on the DCS only for relatively fast projectiles, with wavelengths of the order of the nuclear radius,

$$R_\mathrm{nuc} \simeq 1.2\, A^{1/3}\ \mathrm{fm} = 2.3\times 10^{-5}\, A^{1/3} a_0 , \tag{56}$$

where A is the mass number of the nucleus. In addition, the effect of the correction terms is limited to relatively large angles, where the DCS is several orders of magnitude smaller than at forward directions, and it is outmatched by the effects of the finite size and structure of the nucleus [25], which are disregarded here. For the purposes of particle transport calculations, which are mostly determined by the DCS at small and intermediate angles, it is justified to neglect the relativistic corrections to the potential when their consideration largely complicates the calculations.

4. Quantum theory of elastic collisions

The wave equation for the motion of the projectile relative to the target atom can be obtained by following the familiar heuristic procedure based on the correspondence principle [26]. We start from the relativistic equation of motion in the CM frame of reference, Eq. (36) (for typographic simplicity, here we remove the prime in the relative position vector, *i.e.*, we set $\mathbf{r} = \mathbf{r}'_1 - \mathbf{r}'_2$),

$$p'^2(r) = p'^2_\mathrm{i} - 2\mu_\mathrm{r} V_\mathrm{ef}(r). \tag{57}$$

The time-independent wave equation for free states (*i.e.*, states with positive energy, $E > 0$) is obtained from the classical equation by making the replacement $\mathbf{p}' \to -\mathrm{i}\hbar\nabla$ and by considering that the resulting operators act on the wave function $\psi(\mathbf{r})$ (see, *e.g.*, Ref. [26])

$$\left(-\frac{\hbar^2}{2\mu_r}\nabla^2 + V_{ef}(r)\right)\psi(\mathbf{r}) = \frac{p_i'^2}{2\mu_r}\psi(\mathbf{r})\,. \tag{58}$$

This wave equation has the same form as the non-relativistic Schrödinger equation that describes the scattering of a particle with the relativistic reduced mass μ_r and initial momentum p_i' by the potential $V_{ef}(r)$. Hence, the wave function $\psi(\mathbf{r})$ and the scattering DCS can be evaluated by using the methods and approximations of non-relativistic quantum theory.

It is interesting to consider the limiting form of Eq. (58) when the mass M_2 of the target atom tends to infinity, so that $\beta_{CM} \simeq 0$ and the CM frame coincides with the L frame. Under these circumstances, $\mathbf{p}_i' = \mathbf{p}_{1i}$, $s \simeq \infty$,

$$\mu_r \simeq c^{-2}\mathcal{W}_{1i} = \gamma_{1i}M_1, \quad \text{with} \quad \gamma_{1i} = \sqrt{1+\left(\frac{p_{1i}}{M_1 c}\right)^2}, \tag{59}$$

$$V_{ef}(r) = V(r)\left[1 - \frac{V(r)}{2\gamma_{1i}M_1c^2}\right], \tag{60}$$

and the wave equation becomes

$$\left(-\frac{\hbar^2}{2\gamma_{1i}M_1}\nabla^2 + V(r)\left[1 - \frac{V(r)}{2\gamma_{1i}M_1c^2}\right]\right)\psi(\mathbf{r}) = \frac{p_{1i}^2}{2\gamma_{1i}M_1}\psi(\mathbf{r}), \tag{61}$$

which, as expected, coincides with the Klein-Gordon (or relativistic Schrödinger) equation for free states of a particle with mass M_1 and initial momentum p_{1i} in the electrostatic potential $V(r)$ [3]. Indeed, our derivation shows that the second term in the effective Klein-Gordon potential (60) has a purely kinematic origin.

4.1. Partial-wave expansion method

The DCS for elastic collisions is determined by the asymptotic behavior of a distorted plane wave, *i.e.*, a solution of the wave equation that at large r behaves as a plane wave plus an outgoing spherical wave. For potentials such that $rV_{ef}(r)$ vanishes at $r = \infty$, the distorted plane wave can be expressed in the form of a partial-wave series

$$\psi_{\mathbf{k}}(\mathbf{r}) = (2\pi)^{-3/2}\frac{1}{kr}\sum_{\ell}(2\ell+1)\,\mathrm{i}^{\ell}\,\exp(\mathrm{i}\delta_\ell)\;F_{k\ell}(r)\,P_\ell(\cos\theta'), \tag{62}$$

where $\mathbf{k} = \mathbf{p}_i'/\hbar$ is the wave vector of the incident projectile, $\theta' = \cos^{-1}(\hat{\mathbf{k}}\cdot\hat{\mathbf{r}})$ is the scattering angle (in CM), $P_\ell(\cos\theta')$ are the Legendre polynomials, and the functions $F_{k\ell}(r)$ are solutions of the radial equation

$$\left[-\frac{\hbar^2}{2\mu_r}\frac{\mathrm{d}^2}{\mathrm{d}r^2} + V_{ef}(r) + \frac{\hbar^2}{2\mu_r}\frac{\ell(\ell+1)}{r^2}\right]F_{k\ell}(r) = \frac{p_i'^2}{2\mu_r}F_{k\ell}(r) \tag{63}$$

normalized so that

$$F_{k\ell}(r) \underset{r\to\infty}{\sim} \sin\left[kr - \ell\frac{\pi}{2} + \delta_\ell\right], \tag{64}$$

where δ_ℓ are the scattering phase-shifts. Purely attractive (repulsive) potentials give positive (negative) phase shifts. The asymptotic form of the distorted plane wave,

$$\psi_{\mathbf{k}}(\mathbf{r}) \underset{r\to\infty}{\sim} (2\pi)^{-3/2}\exp(\mathrm{i}\mathbf{k}\cdot\mathbf{r}) + (2\pi)^{-3/2}\frac{\exp(\mathrm{i}kr)}{r}f(\theta'), \tag{65}$$

defines the *scattering amplitude*, $f(\theta')$, which admits the following partial-wave expansion

$$f(\theta') = \frac{1}{2\mathrm{i}k}\sum_{\ell}(2\ell+1)\,[\exp(2\mathrm{i}\delta_\ell) - 1]\,P_\ell(\cos\theta'). \tag{66}$$

The DCS (in CM) is given by

$$\frac{\mathrm{d}\sigma'}{\mathrm{d}\Omega'} = \left|f(\theta')\right|^2. \tag{67}$$

The case of scattering by the Coulomb potential, Eq. (43), is of fundamental importance to understand global properties of atomic collisions. The wave equation (58) for this potential can be solved analytically by using parabolic coordinates [12]. The Coulomb scattering amplitude is given by

$$f_C(\theta') = -\eta\,\frac{\Gamma(1+\mathrm{i}\eta)}{\Gamma(1-\mathrm{i}\eta)}\,\frac{\exp[-\mathrm{i}\eta\ln(\sin^2(\theta'/2))]}{2k\sin^2(\theta'/2)}, \tag{68}$$

where $\Gamma(x)$ is the complex Gamma function and η is the Sommerfeld parameter, Eq. (54). The DCS for scattering by the Coulomb potential is

$$\frac{\mathrm{d}\sigma'_{\mathrm{C}}}{\mathrm{d}\Omega'} = \left|f_{\mathrm{C}}(\theta')\right|^2 = \left(\frac{\mu_{\mathrm{r}} Z_1 Z e^2}{2p'^2_{\mathrm{i}}}\right)^2 \frac{1}{\sin^4(\theta'/2)}. \tag{69}$$

Interestingly, this expression is identical to the classical Rutherford DCS, Eq. (52). This is a fortunate peculiarity of the Coulomb potential; for other potentials the classical and quantum theories yield different DCSs, except when the classical approximation is valid.

4.2. The plane-wave Born approximation

The simplest approach for describing elastic collisions is provided by the plane-wave Born approximation, which is studied in most textbooks on quantum mechanics. Within this approximation, the states of the projectile before and after the collision are represented as plane waves,

$$\phi_{\mathbf{k}}(\mathbf{r}) = (2\pi)^{-3/2} \exp(\mathrm{i}\mathbf{k}\cdot\mathbf{r}), \tag{70}$$

with respective linear momenta $\mathbf{p}'_{\mathrm{i}} = \hbar k\,\hat{\mathbf{z}}$ and $\mathbf{p}'_{\mathrm{f}} = \hbar k\,\hat{\mathbf{k}}_{\mathrm{f}}$, where the unit vector $\hat{\mathbf{k}}_{\mathrm{f}}$ is at an angle θ' from the z axis. The DCS is obtained by considering the potential $V_{\mathrm{ef}}(r)$ as a perturbation to first order, as dictated by Fermi's golden rule [27]. It is given by

$$\frac{\mathrm{d}\sigma'^{(\mathrm{B})}}{\mathrm{d}\Omega'} = \left|f^{(\mathrm{B})}(\theta')\right|^2 \tag{71}$$

with the Born scattering amplitude

$$f^{(\mathrm{B})}(\theta') = -\frac{\mu_{\mathrm{r}}}{2\pi\hbar^2}\int \exp(\mathrm{i}\mathbf{q}\cdot\mathbf{r}/\hbar) V_{\mathrm{ef}}(r)\,\mathrm{d}\mathbf{r} = -\frac{2\mu_{\mathrm{r}}}{\hbar^2}\int_0^\infty \frac{\sin(qr/\hbar)}{qr/\hbar} V_{\mathrm{ef}}(r)\, r^2 \mathrm{d}r, \tag{72}$$

where $\mathbf{q} \equiv \mathbf{p}'_{\mathrm{i}} - \mathbf{p}'_{\mathrm{f}}$ is the momentum transfer, and

$$q = 2p'_{\mathrm{i}} \sin(\theta'/2), \tag{73}$$

is its magnitude. In the case of screened atomic potentials, the Born approximation is valid for projectiles with sufficiently high energies [12].

Introducing the expansion of the plane wave in spherical harmonics [Eq. (4.31) in Ref. [12]], the Born scattering amplitude can be expressed in the form of a partial-wave series as

$$f^{(\mathrm{B})}(\theta') = \frac{1}{2\mathrm{i}k}\sum_{\ell}(2\ell+1)\,(2\mathrm{i}\delta^{(\mathrm{B})}_{\ell})\,P_\ell(\cos\theta')\,, \tag{74}$$

where

$$\delta^{(\mathrm{B})}_{\ell} = -\frac{2\mu_{\mathrm{r}}}{\hbar^2} k \int_0^\infty j^2_\ell(kr) V_{\mathrm{ef}}(r) r^2\,\mathrm{d}r \tag{75}$$

is the Born approximation for the phase shifts.

Although the Born scattering amplitude with the effective potential (38) can be calculated numerically, to obtain simple analytical results we disregard here the relativistic correction terms. In fact, our motivation for considering screened atomic potentials of the form (5) is that they lead to the following simple expressions for the Born scattering amplitude,

$$f^{(\mathrm{B})}(\theta') = -\frac{2\mu_{\mathrm{r}}}{\hbar^2} Z_1 Z e^2 \sum_i A_i \frac{1}{\alpha_i^2 + q^2}, \tag{76}$$

and the Born DCS,

$$\frac{\mathrm{d}\sigma'^{(\mathrm{B})}}{\mathrm{d}\Omega'} = \left|f^{(\mathrm{B})}(\theta')\right|^2 = \left(\frac{2\mu_{\mathrm{r}}}{\hbar^2} Z_1 Z e^2\right)^2 \left(\sum_i A_i \frac{1}{\alpha_i^2 + q^2}\right)^2. \tag{77}$$

If we set $\alpha_i = 0$, we obtain the DCS for Coulomb scattering within the plane-wave Born approximation,

$$\frac{\mathrm{d}\sigma'^{(\mathrm{B})}_{\mathrm{C}}}{\mathrm{d}\Omega'} = \left(\frac{2\mu_{\mathrm{r}}}{\hbar^2} Z_1 Z e^2\right)^2 \frac{1}{q^2} = \left(\frac{\mu_{\mathrm{r}} Z_1 Z e^2}{2p'^2_{\mathrm{i}}}\right)^2 \frac{1}{\sin^4(\theta'/2)}\,, \tag{78}$$

which, again, coincides with the classical Rutherford DCS, Eq. (52).

A further advantage of using the analytical atomic potentials (5) is that their Born phase shifts can be calculated easily with the aid of the equality [Ref. [28], Eq. 6.612.3]

$$\int_0^\infty \exp(-\alpha r)\, j^2_\ell(kr) r\, dr = \frac{1}{2k^2} Q_\ell\left(1 + \frac{\alpha^2}{2k^2}\right), \tag{79}$$

Table 1
Phase shifts for scattering of 10 keV electrons by the DHFS potential of gold atoms ($Z = 79$). WKB phase shifts were calculated for orders $\ell \leq L = 51$. The eikonal phase shifts, $\delta_\ell^{(\mathrm{eik})} = \chi(b)/2$, were calculated from Eq. (91) with $b = (\ell + 1/2)/k$.

	δ_ℓ				
ℓ	numerical	Eqs. (84)	WKB	Born	eikonal
0	6.25076E+0	6.26033E+0	6.26033E+0	7.09519E+0	1.03652E+1
1	4.85210E+0	4.86682E+0	4.86682E+0	4.45239E+0	5.57539E+0
2	3.72213E+0	3.73702E+0	3.73702E+0	3.27638E+0	3.86014E+0
3	2.90479E+0	2.91414E+0	2.91414E+0	2.56871E+0	2.92794E+0
4	2.32614E+0	2.33168E+0	2.33168E+0	2.08362E+0	2.32516E+0
5	1.90282E+0	1.90641E+0	1.90641E+0	1.72640E+0	1.89705E+0
6	1.58154E+0	1.58402E+0	1.58402E+0	1.45153E+0	1.57569E+0
7	1.33066E+0	1.33243E+0	1.33243E+0	1.23382E+0	1.32587E+0
8	1.13061E+0	1.13189E+0	1.13189E+0	1.05782E+0	1.12698E+0
9	9.68531E-1	9.69443E-1	9.69443E-1	9.13385E-1	9.65866E-1
10	8.35528E-1	8.36179E-1	8.36179E-1	7.93454E-1	8.33608E-1
15	4.32699E-1	4.32795E-1	4.32795E-1	4.20759E-1	4.32321E-1
20	2.46941E-1	2.46926E-1	2.46926E-1	2.43066E-1	2.46832E-1
25	1.50843E-1	1.50813E-1	1.50813E-1	1.49433E-1	1.50792E-1
30	9.68752E-2	9.68507E-2	9.68507E-2	9.63097E-2	9.68454E-2
35	6.45745E-2	6.45571E-2	6.45571E-2	6.43283E-2	6.45556E-2
40	4.42433E-2	4.42315E-2	4.42315E-2	4.41288E-2	4.42310E-2
50	2.19469E-2	2.19412E-2	2.19412E-2	2.19184E-2	2.19412E-2
75	4.44078E-3	4.43988E-3	-----	4.43947E-3	4.43932E-3
100	9.76997E-4	9.76935E-4	-----	9.76927E-4	9.76527E-4
150	5.15943E-5	5.15950E-5	-----	5.15950E-5	5.15523E-5
200	2.88128E-6	2.88181E-6	-----	2.88181E-6	2.87841E-6
250	1.65537E-7	1.65995E-7	-----	1.65996E-7	1.65742E-7

where $Q_\ell(x)$ are the Legendre functions of the second kind [29]. We have

$$\delta_\ell^{(\mathrm{B})} = -\frac{\mu_\mathrm{r}}{\hbar^2 k} Z_1 Z e^2 \sum_i A_i Q_\ell\left(1 + \frac{\alpha_i^2}{2k^2}\right). \tag{80}$$

The functions $Q_\ell(r)$ are calculated by using the strategy described by Fernández-Varea et al. [30].

4.3. Approximate phase shifts

Generally, the Born phase shifts (75) provide a good approximation to the actual phase shifts that are small in magnitude, even when the Born approximation for the scattering amplitude is not accurate. To allow the calculation of the scattering amplitude from the partial-wave series (66) we need an alternative method to obtain those phase shifts that are not small. We use the Wentzel-Kramers-Brillouin (WKB) approximation, with the Langer correction, which leads to the following formula for the phase shifts [12]

$$\delta_\ell^{(\mathrm{WKB})} = \frac{1}{2}\left(\ell + \frac{1}{2}\right)\pi - k r_0 + \int_{r_0}^{\infty} \left[\sqrt{F_\ell(r)} - k\right] \mathrm{d}r \tag{81}$$

where

$$F_\ell(r) = k^2 - \frac{2\mu_\mathrm{r}}{\hbar^2} V_\mathrm{ef}(r) - \frac{(\ell + 1/2)^2}{r^2}, \tag{82}$$

and r_0 is the largest zero of $F_\ell(r)$. The WKB approximation is accurate when the potential $V_\mathrm{ef}(r)$ is practically constant over many wavelengths or, more precisely, when [3]

$$\left|\frac{1}{2F_\ell(r)} \frac{\mathrm{d}}{\mathrm{d}r}\sqrt{F_\ell(r)}\right| \ll 1 \qquad \text{for } r > r_0. \tag{83}$$

It is convenient to have a feel of the accuracy of the WKB and Born approximations for the phase shifts. In the case of electrons or positrons, the program RADIAL [20] gives accurate phase shifts obtained from the numerical solution of the radial equation (63), which is integrated by using a robust power-series solution method. The accuracy of WKB and Born phase shifts can then be estimated by comparison with the numerical values generated by RADIAL. A similar comparison of approximate and numerical phase shifts for projectiles heavier than the electron is not possible because the small wavelengths of these particles make the numerical calculation of phase shifts very lengthy. As a matter of fact, the study for electrons is sufficient for our purposes because the WKB approximation at a given energy is more accurate for the heavier particles, due to their shorter wave lengths.

Table 1 shows phase-shifts obtained from the WKB and Born approximations (as given by the program ECCPA) and "exact" phase shifts given by the code RADIAL, for the case of scattering of 10 keV electrons by gold atoms ($Z = 79$), with all phase shifts calculated by using the analytical DHFS potential (Section 2), *i.e.*, by neglecting the relativistic corrections (39). To be consistent with the RADIAL calculation, the approximate phase shifts were calculated with the reduced mass equal to the electron mass $\mathrm{m_e}$ and a linear momentum $p_\mathrm{i} = (2\mathrm{m_e}E)^{1/2}$. The WKB phase shifts are in fairly good agreement with the numerical values; relative differences are of the order of 1% for $\ell = 0$, and generally the differences are smaller for larger ℓ. The Born phase-shifts of small angular momenta ℓ are less accurate

than the WKB phase shifts; the relative differences between the WKB and Born phases decrease progressively when ℓ increases. Beyond a certain ℓ, the Born phase shifts give an acceptable approximation to the actual phase shifts. For projectiles with higher energies we find the same tendencies, except that the phase shifts decrease in magnitude more slowly with ℓ. That is, the convergence of the partial-wave series slows down when the energy increases.

The differences between numerical and approximate phase shifts of low orders are the most relevant, because they amount to adding or subtracting a smooth component to the DCS, whose effect is magnified at large angles, where the actual DCS is smaller. Indeed, since the Legendre polynomial $P_\ell(\cos\theta')$ has ℓ zeros nearly uniformly spaced, an error in the ℓ-th order phase shift will manifest as an oscillation of the calculated DCS with respect to the "correct" DCS with nearly ℓ crests and troughs of similar amplitude.

Guided by these observations, and considering that the coefficients in the Legendre series of the actual scattering amplitude vary smoothly with ℓ, we set

$$\delta_\ell = \begin{cases} \delta_\ell^{(\mathrm{WKB})} & \text{if } \ell < L, \\ C_\ell \delta_\ell^{(\mathrm{B})} & \text{otherwise,} \end{cases} \tag{84a}$$

where the cutoff order L is the lowest value of ℓ for which either $\delta_\ell^{(\mathrm{B})} < 0.001$ or the relative difference between the WKB and Born phase shifts is less than 0.001. Evidently, this prescription implies that only WKB phase shifts of orders $\ell \leq L$ need to be computed. The factor

$$C_\ell \equiv 1 + \left(\frac{\delta_L^{(\mathrm{WKB})}}{\delta_L^{(\mathrm{B})}} - 1 \right) \exp\left(-a\, \frac{\ell - L}{L} \right) \tag{84b}$$

is introduced to ensure that the approximate phase shifts δ_ℓ vary smoothly with ℓ near the cutoff L. The form of this factor, which has been decided on the basis of the observed variation of the difference between the WKB and Born phase shifts with ℓ, is practically irrelevant as long as it ensures "continuity" at $\ell = L$ and tends to unity at large ℓ, where the Born approximation to the phase shifts is expected to be valid. The parameter a is obtained by requiring that $\delta_{L-1}^{(\mathrm{WKB})} = C_{L-1}\delta_{L-1}^{(\mathrm{B})}$, with the proviso that the relative difference of δ_ℓ and $\delta_\ell^{(\mathrm{B})}$ effectively decreases with ℓ. Omission of the factor C_ℓ may cause the scattering amplitude to oscillate about its "average" shape with a frequency depending on the cutoff order L and an amplitude proportional to the magnitude of the "discontinuity" between WKB and Born phase shifts.

As mentioned above, the convergence of the partial-wave series may be very slow. We can alleviate the numerical work by adding the Born scattering amplitude and subtracting its partial-wave expansion,

$$f(\theta') = f^{(\mathrm{B})}(\theta') + \frac{1}{2\mathrm{i}k} \sum_{\ell=0}^{\infty} (2\ell+1) \left[\exp(2\mathrm{i}\delta_\ell) - 1 - 2\mathrm{i}\delta_\ell^{(\mathrm{B})} \right] P_\ell(\cos\theta') \tag{85}$$

Since the phase shifts δ_ℓ approximate the Born phase shifts when $\ell \gtrsim L$, this series converges more rapidly than the original series (66). For scattering angles larger than about 1 degree, convergence is further improved by applying the "reduced series" method [31,32], which exploits the fact that, if a function $f(\theta')$ is strongly peaked at $\theta' = 0$, the function $(1 - \cos\theta') f(\theta')$ is smoother than $f(\theta')$ and, hence, its Legendre expansion is expected to converge more rapidly.

4.4. The eikonal approximation

An alternative description of elastic collisions, valid for projectiles with sufficiently high energies and at small angles, is provided by the so-called eikonal approximation [3,17], in which the phase of the scattered wave is obtained from a semi-classical approach under the assumption of small trajectory deflections. A detailed derivation of the wave function within the eikonal approximation and the corresponding scattering amplitude is given in Joachain's book [12]. Here we present an alternative derivation based on Molière's [17] observation that the eikonal scattering amplitude can be obtained as the small-angle limit of the partial-wave expansion (66) with the phase shifts calculated from the WKB approximation, Eq. (81). To determine the small-angle limit of the partial-wave expansion, we notice that the WKB phase shifts vanish for $V_{\mathrm{ef}}(r) = 0$ because

$$\frac{1}{2}\left(\ell + \frac{1}{2}\right)\pi - kb = -\int_b^\infty \left[\sqrt{k^2 - \frac{(\ell+1/2)^2}{r^2}} - k \right] \mathrm{d}r, \tag{86}$$

where

$$b = \frac{\ell + 1/2}{k} \tag{87}$$

is the classical impact parameter corresponding to the angular momentum $\ell + \frac{1}{2}$; the additional $\frac{1}{2}$ in the WKB formulas occurs as a consequence of the fact that the radial motion is limited to positive values of r [33]. We can then write

$$\begin{aligned} \delta_\ell^{(\mathrm{WKB})} &= \int_{r_0}^\infty \left[\sqrt{k^2 - \frac{2\mu_\mathrm{r}}{\hbar^2} V_{\mathrm{ef}}(r) - \frac{(\ell+1/2)^2}{r^2}} - k \right] \mathrm{d}r - \int_b^\infty \left[\sqrt{k^2 - \frac{(\ell+1/2)^2}{r^2}} - k \right] \mathrm{d}r \\ &= \int_b^\infty \left[\sqrt{K^2(r) - \frac{2\mu_\mathrm{r}}{\hbar^2} V_{\mathrm{ef}}(r)} - K(r) \right] \mathrm{d}r - \int_{r_0}^b \left[\sqrt{k^2 - \frac{2\mu_\mathrm{r}}{\hbar^2} V_{\mathrm{ef}}(r) - \frac{(\ell+1/2)^2}{r^2}} - k \right] \mathrm{d}r \end{aligned} \tag{88}$$

with

$$K^2(r) = k^2 - \frac{(\ell+1/2)^2}{r^2} = k^2\left(1 - \frac{b^2}{r^2}\right). \tag{89}$$

Small angles generally correspond to relatively large impact parameters b so that $V_{\rm ef}(r)$ is much smaller than $K(r)$ for $r > b$ and r_0 tends to b when ℓ increases. Consequently, for sufficiently large b or ℓ, we can neglect the second integral in Eq. (88), and approximate the first term in that expression by expanding the square root in powers of $V_{\rm ef}/K^2$. Neglecting terms of second and higher orders, we obtain the eikonal approximation for the phase shifts,

$$\delta_\ell^{(\rm eik)} = -\frac{\mu_{\rm r}}{\hbar^2}\int_b^\infty \frac{V_{\rm ef}(r)}{K(r)}\,{\rm d}r = -\frac{\mu_{\rm r}}{\hbar^2 k}\int_b^\infty V_{\rm ef}(r)\,\frac{r\,{\rm d}r}{\sqrt{r^2-b^2}} \equiv \tfrac{1}{2}\chi(b), \tag{90}$$

where $\chi(b)$ is the eikonal phase function. The foregoing derivation indicates that this formula is expected to be valid (*i.e.*, to give results close to the exact values of the phase shifts) for large ℓ's.

Wallace [34] derived systematic corrections of order k^{-n} to the eikonal phase. With the first-order Wallace correction included, the eikonal phase is

$$\chi(b) = -\frac{2\mu_{\rm r}}{\hbar^2 k}\int_b^\infty V_{\rm ef}(r)\left\{1 + \frac{\mu_{\rm r}}{\hbar^2 k^2}\left[V_{\rm ef}(r) + r\,\frac{{\rm d}V_{\rm ef}(r)}{{\rm d}r}\right]\right\}\frac{r\,{\rm d}r}{\sqrt{r^2-b^2}}. \tag{91}$$

In the limit of high energies, the factor in curly braces, the Wallace correction, tends to unity and the expression (91) reduces to the form (90). Byron and Joachain [35] have analyzed the reliability of the eikonal approximation for screened atomic potentials, and concluded that Wallace's correction does improve the accuracy of the method. The eikonal phase shifts for 10 keV electrons scattered by the DHFS potential of the free gold atom (with the Wallace correction and $V_{\rm ef} = V$) are shown in Table 1. Notice that the relative difference between phase shifts calculated with the WKB method and with the eikonal approximation decreases rapidly when the angular momentum increases.

The following approximation to the Legendre polynomials [17]

$$P_\ell(\cos\theta') \simeq \sqrt{\frac{\theta'}{\sin\theta'}}\,J_0\left(\frac{2\ell+1}{2}\,\theta'\right) \tag{92}$$

is valid for any $\theta' < \pi$ in the limit for large ℓ, and for all values of ℓ in the limit for small θ'. Inserting the approximations (90) and (92) into the partial-wave expansion (66) of the scattering amplitude, and replacing the summation over $\ell = kb - \frac{1}{2}$ with an integral, we have

$$f(\theta') \simeq \frac{1}{2{\rm i}k}\int_0^\infty {\rm d}(kb)\,2kb\,\{\exp[{\rm i}\chi(b)] - 1\}\sqrt{\frac{\theta'}{\sin\theta'}}\,J_0\left(kb\,\theta'\right).$$

Hence, for small angles (such that $\sin\theta' \simeq \theta'$, $q \simeq \hbar k\theta'$) we can write

$$f(\theta') \simeq -{\rm i}k\int_0^\infty \{\exp[{\rm i}\chi(b)] - 1\}\,J_0(qb/\hbar)\,b\,{\rm d}b, \tag{93}$$

which is the eikonal scattering amplitude [12,17].

For atomic potentials of the form (5), the eikonal phase (91) can be calculated analytically as [36,37]

$$\chi(b) = -\frac{2\mu_{\rm r} Z_1 Z e^2}{\hbar^2 k}\sum_i A_i\left\{K_0(a_i b) - \frac{\mu_{\rm r} Z_1 Z e^2}{\hbar^2 k^2}\sum_j A_j a_j K_0[(a_i + a_j)b]\right\}, \tag{94}$$

where $K_0(x)$ is the modified Bessel function of the second kind and zeroth order. The evaluation of the expression (93) thus reduces to a single quadrature, which must be performed numerically. To ease the calculation we follow Zeitler and Olsen [38] and, instead of directly evaluating the integral (93), we use the equivalent expression

$$f^{(\rm eik)}(\theta') = -\frac{\hbar k}{q}\int_0^\infty J_1(qb/\hbar)\,\frac{{\rm d}\chi(b)}{{\rm d}b}\,\exp\left[{\rm i}\chi(b)\right]b\,{\rm d}b. \tag{95}$$

The derivative of the eikonal phase (94) is

$$\frac{{\rm d}\chi(b)}{{\rm d}b} = \frac{2\mu_{\rm r} Z_1 Z e^2}{\hbar^2 k}\sum_i A_i\left\{a_i K_1(a_i b) - \frac{\mu_{\rm r} Z_1 Z e^2}{\hbar^2 k^2}\sum_j A_j a_j (a_i + a_j) K_1[(a_i + a_j)b]\right\}, \tag{96}$$

where $K_1(x)$ is the modified Bessel function of the second kind and first order. The integral (95) converges rapidly for large values of b because of the exponentially decaying $K_1(a_i b)$, and the fast oscillations of the exponential at small b are suppressed by the $J_1(qb)$ function, which vanishes at $b = 0$. The DCS is given by

$$\frac{\mathrm{d}\sigma'^{(\mathrm{eik})}}{\mathrm{d}\Omega'} = |f^{(\mathrm{eik})}(\theta')|^2. \tag{97}$$

The eikonal approximation is expected to be accurate for scattering angles up to about $(kR)^{-1}$ [17], where R is the atomic radius, Eq. (9). However, numerical calculations indicate that for protons and heavier particles the approximation yields fairly accurate DCSs, practically coincident with those obtained from classical and partial-wave calculations up to much larger angles, of the order of

$$\theta'_{\mathrm{eik}} = \min\left\{\frac{200}{kR}, 0.1\pi\right\}. \tag{98}$$

For angles somewhat larger than θ'_{eik}, the calculation presents numerical instabilities and must be discontinued. In the computer program ECCPA the DCS for $\theta' > \theta'_{\mathrm{eik}}$ is estimated by extrapolation using the empirical formula proposed by Salvat [37],

$$\frac{\mathrm{d}\sigma'^{(\mathrm{eik})}}{\mathrm{d}\Omega'} = \left(\frac{2\mu_{\mathrm{r}}}{\hbar^2} Z_1 Z e^2\right)^2 \frac{1}{\left[A + Bq^{2/3} + Cq^{4/3} + q^2\right]^2}, \tag{99}$$

with the coefficients A, B and C determined by matching the calculated numerical values of the eikonal DCS and its first and second derivatives at $\theta' = \theta'_{\mathrm{eik}}$. In the case of proton collisions, the extrapolated DCS differs by less than about 1% from the classical DCS, which is expected to be accurate for large scattering angles. Note that for momentum transfers that are large enough, both the Born DCS and the extrapolated eikonal DCS tend to the Rutherford DCS (52), which decreases rapidly with the scattering angle ($\propto q^{-4}$).

5. Cross sections in the L frame

In the foregoing Sections, the DCS is calculated in the CM frame. The total cross section,

$$\sigma' = \int \frac{\mathrm{d}\sigma'}{\mathrm{d}\Omega'}\,\mathrm{d}\Omega', \tag{100}$$

and the momentum transfer cross section, also called the first transport cross section,

$$\sigma_{\mathrm{mt}} = \int (1 - \cos\theta')\frac{\mathrm{d}\sigma'}{\mathrm{d}\Omega'}\,\mathrm{d}\Omega', \tag{101}$$

can be calculated numerically as integrals of the DCS. Alternatively, they can evaluated from the partial-wave expansion of the scattering amplitude, by using the orthogonality properties of the Legendre polynomials,

$$\sigma' = \frac{4\pi}{k^2}\sum_{\ell=0}^{\infty}(2\ell+1)\sin^2(\delta_\ell), \tag{102}$$

and

$$\sigma_{\mathrm{mt}} = \frac{4\pi}{k^2}\sum_{\ell}(\ell+1)\,\sin^2(\delta_\ell - \delta_{\ell+1}). \tag{103}$$

It is worth mentioning that the results from partial-wave calculations (and from the eikonal approximation) satisfy the optical theorem (see, *e.g.*, Refs. [3], [12]),

$$\sigma' = \frac{4\pi}{k}\,\mathrm{Im}\,f(0). \tag{104}$$

This equality is a direct consequence of the conservation of probability (collisions neither produce nor absorb projectiles).

The four-momenta of a particle in the L and CM frames are related by the Lorentz transformation equations (17). The polar and azimuthal angles of its directions of motion in the two frames are related by [see, *e.g.*, Ref. [22], Eq. (11.32)]

$$\phi = \phi', \qquad \tan\theta = \frac{1}{\gamma_{\mathrm{CM}}}\,\frac{\sin\theta'}{\tau + \cos\theta'} \tag{105}$$

with $\tau = v_{\mathrm{CM}}/v'$, where v_{CM} and $v' = c^2 p'/W'$ are, respectively, the velocities of the CM and of the particle in CM. The second equality in (105) may be expressed in the equivalent form

$$\cos\theta = \frac{\tau + \cos\theta'}{\sqrt{(\tau + \cos\theta')^2 + \gamma_{\mathrm{CM}}^{-2}\sin^2\theta'}}. \tag{106}$$

The inverse relation is

$$\cos\theta' = \frac{-\tau_1\gamma_{\mathrm{CM}}^2\sin^2\theta_1 \pm \cos\theta_1\sqrt{\cos^2\theta_1 + \gamma_{\mathrm{CM}}^2(1-\tau_1^2)\sin^2\theta_1}}{\gamma_{\mathrm{CM}}^2\sin^2\theta_1 + \cos^2\theta_1}. \tag{107}$$

When $\tau < 1$ only the plus sign is valid and θ increases monotonically with θ', that is, there is a unique correspondence between θ and θ'. When $\tau \geq 1$, the angle θ in the L frame can only take values in the interval from 0 to the value

$$\theta_{\max} = \arccos\left(\frac{1}{\sqrt{1+\gamma_{\rm CM}^{-2}(\tau^2-1)^{-1}}}\right). \tag{108}$$

In addition, if $\tau \geq 1$ each angle $\theta \leq \theta_{\max}$ corresponds to two different angles in CM, which are given by the formula (107) with the plus and minus signs.

The DCS in the L frame is

$$\frac{{\rm d}\sigma}{{\rm d}\Omega} = \left|\frac{{\rm d}(\cos\theta')}{{\rm d}(\cos\theta_1)}\right| \frac{{\rm d}\sigma'}{{\rm d}\Omega'} = \frac{\gamma_{\rm CM}^2\left[\tau\cos\theta \pm \sqrt{\cos^2\theta + \gamma_{\rm CM}^2(1-\tau^2)\sin^2\theta}\,\right]^2}{\left(\gamma_{\rm CM}^2\sin^2\theta+\cos^2\theta\right)^2\sqrt{\cos^2\theta_1+\gamma_{\rm CM}^2(1-\tau^2)\sin^2\theta}}\,\frac{{\rm d}\sigma_1'}{{\rm d}\Omega'}, \tag{109}$$

with

$$\tau = \frac{v_{\rm CM}}{v_1'} = \frac{\beta_{\rm CM}W_1'}{cp_1'} \tag{110}$$

If $\tau < 1$ only the plus sign is valid and the scattering angle θ varies from 0 to π. When $\tau \geq 1$ the DCS vanishes for $\theta > \theta_{\max}$; for angles θ less than $\theta_{\max}$, Eq. (108) yields two values of θ' in $(0,\pi)$, the expression on the right-hand side of Eq. (109) must then be evaluated for these two angles, and the resulting values added up to give the DCS in L. Evidently, the total cross section in L is the same as in CM.

In calculations of stopping of charged particles in matter, it is natural to consider the DCS differential in the energy loss of the projectile, $\Delta E = E_{1\rm i} - E_{1\rm f}$. Energy-momentum conservation implies that

$$\Delta E = (\Delta E)_{\max}\,\frac{1-\cos\theta'}{2} \tag{111}$$

with

$$(\Delta E)_{\max} = \frac{M_2c^4p_{1\rm i}^2}{\mathcal{S}^2} = \frac{2M_2c^2\,E_{1\rm i}(E_{1\rm i}+2M_1c^2)}{(M_1c^2+M_2c^2)^2+2M_2c^2E_{1\rm i}}\,. \tag{112}$$

Hence

$$\frac{{\rm d}\sigma}{{\rm d}(\Delta E)} = \frac{{\rm d}\sigma'}{{\rm d}\Omega'}\,2\pi\left|\frac{{\rm d}(\Delta E)}{{\rm d}(\cos\theta')}\right|^{-1} = \frac{4\pi}{(\Delta E)_{\max}}\,\frac{{\rm d}\sigma'}{{\rm d}\Omega'}\,. \tag{113}$$

The stopping cross section is

$$\sigma_{\rm st} \equiv \int_0^{(\Delta E)_{\max}} \Delta E\,\frac{{\rm d}\sigma}{{\rm d}(\Delta E)}\,{\rm d}(\Delta E) = \frac{(\Delta E)_{\max}}{2}\,2\pi\int_{-1}^{1}(1-\cos\theta')\,\frac{{\rm d}\sigma'}{{\rm d}\Omega'}\,{\rm d}(\cos\theta')$$

$$= \frac{(\Delta E)_{\max}}{2}\,\sigma_{\rm mt}\,, \tag{114}$$

where $\sigma_{\rm mt}$ is the momentum-transfer cross section, Eq. (101). The average energy transfer in a collision is

$$\langle\Delta E\rangle = \frac{\sigma_{\rm st}}{\sigma} = \frac{(\Delta E)_{\max}}{2}\,\frac{\sigma_{\rm mt}}{\sigma}\,. \tag{115}$$

6. Collisions of electrons and positrons

Electrons and positrons (mass $M_1 = {\rm m_e}$ and charge Z_1e, $Z_1 = \pm 1$) are peculiar in that they have spin 1/2 and their mass is much smaller than those of other charged particles. The relativistic wave equation of the electron and the positron in an external potential is the Dirac equation [11,26,39]. Although elastic scattering of these particles can be accurately calculated by means of numerical Dirac partial-wave analysis using available computer codes [8,20], the process provides a unique benchmark to assess the accuracy of the Born and WKB approximations for the phase shifts. Because of the small mass of the electron, the recoil of the target atom is negligible, and calculations can be performed in the L frame. Here we consider collisions of a spin 1/2 projectile with momentum $p = \hbar k$ with a target atom, assumed to be at rest at the origin of the L frame.

The scattering of Dirac particles by a central potential $V(r)$ is completely described by the direct scattering amplitude, $f(\theta)$, and the spin-flip scattering amplitude, $g(\theta)$. These are complex functions of the polar scattering angle θ determined from the large-r behavior of the Dirac distorted waves, *i.e.*, the solutions of the Dirac equation for the central potential $V(r)$ that behave asymptotically as a plane wave plus an outgoing spherical wave [11,39]. The scattering amplitudes admit the following partial-wave expansions

$$f^{(\rm D)}(\theta) = \frac{1}{2{\rm i}k}\sum_{\ell=0}^{\infty}\Big\{(\ell+1)\left[\exp\left(2{\rm i}\delta_{\kappa=-\ell-1}\right)-1\right] + \ell\left[\exp\left(2{\rm i}\delta_{\kappa=\ell}\right)-1\right]\Big\}\,P_\ell(\cos\theta) \tag{116a}$$

and

$$g^{(\mathrm{D})}(\theta) = \frac{1}{2\mathrm{i}k}\sum_{\ell=0}^{\infty}\left[\exp\left(2\mathrm{i}\delta_{\kappa=-\ell-1}\right) - \exp\left(2\mathrm{i}\delta_{\kappa=\ell}\right)\right] P_\ell^1(\cos\theta), \tag{116b}$$

where $P_\ell(\cos\theta)$ and $P_\ell^1(\cos\theta)$ are Legendre polynomials and associated Legendre functions, respectively. The DCS for elastic collisions of spin-unpolarized projectiles is given by [11,40]

$$\frac{\mathrm{d}\sigma^{(\mathrm{D})}}{\mathrm{d}\Omega} = |f^{(\mathrm{D})}(\theta)|^2 + |g^{(\mathrm{D})}(\theta)|^2. \tag{117}$$

The phase shifts δ_κ are determined by the large-r behavior of the radial wave functions $P_{E\kappa}(r)$ and $Q_{E\kappa}(r)$, which satisfy the radial Dirac equations [39]

$$\frac{\mathrm{d}P_{E\kappa}}{\mathrm{d}r} = -\frac{\kappa}{r}P_{E\kappa} + \frac{E - V + 2M_1c^2}{c\hbar}Q_{E\kappa},$$

$$\frac{\mathrm{d}Q_{E\kappa}}{\mathrm{d}r} = -\frac{E - V}{c\hbar}P_{E\kappa} + \frac{\kappa}{r}Q_{E\kappa}, \tag{118}$$

where E is the kinetic energy of the projectile,

$$E = M_1c^2\left[\sqrt{1 + \left(\frac{p}{M_1c}\right)^2} - 1\right]. \tag{119}$$

The upper-component radial function $P_{E\kappa}(r)$ oscillates asymptotically as

$$P_{E\kappa}(r) \simeq \sin\left(kr - \ell\frac{\pi}{2} + \delta_\kappa\right), \tag{120}$$

where δ_κ is the phase shift. As in the case of spinless particles, attractive (repulsive) potentials give positive (negative) phase shifts.

6.1. The Dirac–Born approximation

The simplest approach for computing scattering DCSs of Dirac particles is provided by the plane-wave Born approximation, which yields the following expressions of the scattering amplitudes for scattering by a central potential $V(r)$ [32,41],

$$f^{(\mathrm{DB})}(\theta) = \left(\frac{\gamma+1}{2} + \frac{\gamma-1}{2}\cos\theta\right) f^{(\mathrm{B})}(\theta), \tag{121a}$$

$$g^{(\mathrm{DB})}(\theta) = \frac{\gamma-1}{2}\sin\theta\, f^{(\mathrm{B})}(\theta), \tag{121b}$$

where

$$\gamma = \frac{E + M_1c^2}{M_1c^2} \tag{122}$$

and $f^{(\mathrm{B})}(\theta)$ is the non-relativistic Born scattering amplitude, Eq. (72). The Dirac–Born DCS for spin-unpolarized projectiles is

$$\frac{\mathrm{d}\sigma^{(\mathrm{DB})}}{\mathrm{d}\Omega} = |f^{(\mathrm{DB})}(\theta)|^2 + |g^{(\mathrm{DB})}(\theta)|^2 = \left[1 - \beta^2\sin^2(\theta/2)\right]\gamma^2\left|f^{(\mathrm{B})}(\theta)\right|^2, \tag{123}$$

with $\beta^2 = 1 - \gamma^{-2}$. The factor $1 - \beta^2\sin^2(\theta/2)$ accounts for the effect of spin, which is mostly caused by the spin-orbit interaction (see, *e.g.*, [42]), and the factor γ^2 accounts for the relativistic increase of the projectile mass.

The DCS for spin 1/2 projectiles can also be calculated by using the classical trajectory method and the eikonal approximation. These approaches disregard the spin of the projectile. To account, at least partially, for the effect of spin, the calculated DCSs are multiplied by the spin factor $1 - \beta^2\sin^2(\theta/2)$.

The Dirac–Born scattering amplitudes (121) can be expressed in the form of Legendre series,

$$f^{(\mathrm{DB})}(\theta) = \frac{1}{k}\sum_{\ell=0}^{\infty}\left[(\ell+1)\delta^{(\mathrm{DB})}_{\kappa=-\ell-1} + \ell\delta^{(\mathrm{DB})}_{\kappa=\ell}\right]P_\ell(\cos\theta), \tag{124a}$$

$$g^{(\mathrm{DB})}(\theta) = \frac{1}{k}\sum_{\ell=0}^{\infty}\left[\delta^{(\mathrm{DB})}_{\kappa=-\ell-1} - \delta^{(\mathrm{DB})}_{\kappa=\ell}\right]P_\ell^1(\cos\theta), \tag{124b}$$

with the Dirac–Born phase shifts

$$\delta^{(\mathrm{DB})}_{\kappa=-\ell-1} = \frac{\gamma+1}{2}\delta^{(\mathrm{B})}_\ell + \frac{\gamma-1}{2}\delta^{(\mathrm{B})}_{\ell+1}, \tag{125a}$$

$$\delta^{(\mathrm{DB})}_{\kappa=\ell} = \frac{\gamma+1}{2}\delta^{(\mathrm{B})}_\ell + \frac{\gamma-1}{2}\delta^{(\mathrm{B})}_{\ell-1}, \tag{125b}$$

where $\delta_\ell^{(\mathrm{B})}$ are the non-relativistic Born phase shifts, Eq. (75). For potentials of the form (5) these phase shifts can be readily evaluated by means of the analytical formula (80). The values so obtained provide a good approximation to the actual phase shifts that are small (*i.e.*, those of large orders $|\kappa|$), even when the Born approximation for the scattering amplitudes is not accurate.

6.2. Approximate Dirac phase shifts

To estimate the phase shifts with relatively large absolute values (those of small orders), we take advantage of the fact that the radial Dirac Eqs. (118) may be reduced to Schrödinger form by introducing the substitution [11,40]

$$P_{E\kappa}(r) = A^{1/2}(r)\mathcal{P}(r), \tag{126}$$

with

$$A(r) \equiv \frac{E - V(r) + 2M_1c^2}{2M_1c^2}, \tag{127}$$

and eliminating the small-component radial function $Q_{E\kappa}(r)$. The resulting equation is

$$\left[-\frac{\hbar^2}{2M_1}\frac{\mathrm{d}^2}{\mathrm{d}r^2} + V_{\mathrm{ef}}^{(\mathrm{D})}(r) + \frac{\hbar^2}{2M_1}\frac{\ell(\ell+1)}{r^2}\right]\mathcal{P}(r) = \frac{p^2}{2M_1}\mathcal{P}(r), \tag{128}$$

where $\ell = \kappa$ if $\kappa > 0$ and $\ell = -\kappa - 1$ if $\kappa < 0$, and the effective Dirac potential,

$$V_{\mathrm{ef}}^{(\mathrm{D})}(r) = V + \frac{1}{2M_1c^2}\left\{V\,(2E - V) + (\hbar c)^2\left[\frac{\kappa}{r}\frac{A'}{A} + \frac{3}{4}\left(\frac{A'}{A}\right)^2 - \frac{1}{2}\frac{A''}{A}\right]\right\}, \tag{129}$$

depends on the energy and the relativistic quantum number κ. For large r values, $A(r)$ becomes a constant, *i.e.*, $\mathcal{P}$ becomes proportional to $P_{E\kappa}$, and therefore the phase shifts may be computed by solving the radial Schrödinger equation (128) as in the non-relativistic case. In particular, the WKB approximation with the Langer correction yields [cf. Eq. (81)]

$$\delta_\kappa^{(\mathrm{WKB})} = \frac{1}{2}\left(\ell + \frac{1}{2}\right)\pi - kr_0 + \int_{r_0}^{\infty}\left[\sqrt{F_\kappa(r)} - k\right]\mathrm{d}r, \tag{130}$$

where

$$F_\kappa(r) = k^2 - \frac{2M_1}{\hbar^2}V_{\mathrm{ef}}^{(\mathrm{D})}(r) - \frac{(\ell + 1/2)^2}{r^2} \tag{131}$$

and r_0 is the largest zero of $F_\kappa(r)$.

The accuracy of WKB and Born approximate phase shifts can be readily assessed by comparison with numerical phase shifts calculated by the computer program RADIAL [20]. Such a comparison shows general trends similar to the case of spinless particles (see Table 1). The WKB phase shifts are in fairly good agreement with the numerical phases; the relative differences are about 1% for $\ell = 0$ and decrease when the order ℓ increases. The Born phase shifts are less accurate than the WKB phases for low ℓ, but they tend progressively to the numerical values when ℓ increases. Consequently, we use the recipe given in Eqs. (84) to define the approximate phase shifts. Thus, for the set of phase shifts with $\kappa < 0$, we define

$$\delta_{\kappa=-\ell-1} = \begin{cases} \delta_{-\ell-1}^{(\mathrm{WKB})} & \text{if } \ell < L, \\ C_{-\ell-1}\delta_{-\ell-1}^{(\mathrm{DB})} & \text{otherwise,} \end{cases} \tag{132a}$$

where the cutoff value L is the lowest value of ℓ for which either $\delta_{-\ell-1}^{(\mathrm{B})} < 0.001$ or the relative difference between the WKB and Born phase shifts is less than 0.001. The factor

$$C_{-\ell-1} = 1 + \left(\frac{\delta_{-L-1}^{(\mathrm{WKB})}}{\delta_{-L-1}^{(\mathrm{DB})}} - 1\right)\exp\left(-a\,\frac{\ell - L}{L}\right), \tag{132b}$$

with the parameter a determined so that the phase shifts $\delta_{\kappa=-\ell-1}$ vary smoothly with ℓ, as described in Section 4.3. Phase shifts with positive κ are defined similarly.

The DCS and the scattering amplitudes for high-energy projectiles are sharply peaked at $\theta = 0$ and, consequently, the convergence of the partial-wave series is quite slow. As in the case of spinless projectiles, convergence is speeded up by adding the Born scattering amplitudes, Eq. (121) and subtracting their partial-wave expansions, Eq. (124). We thus obtain

$$f^{(\mathrm{D})}(\theta) = f^{(\mathrm{DB})}(\theta) + \sum_{\ell=0}^{\infty}\mathcal{F}_\ell\,P_\ell(\cos\theta) \tag{133a}$$

and

$$g^{(\mathrm{D})}(\theta) = g^{(\mathrm{DB})}(\theta) + \sum_{\ell=0}^{\infty} \mathcal{G}_\ell \, P_\ell^1(\cos\theta), \tag{133b}$$

where

$$\mathcal{F}_\ell = \frac{1}{2\mathrm{i}k}\Big\{(\ell+1)\left[\exp\left(2\mathrm{i}\delta_{\kappa=-\ell-1}\right)-1\right] + \ell\left[\exp\left(2\mathrm{i}\delta_{\kappa=\ell}\right)-1\right]\Big\} - \frac{1}{k}\left[(\ell+1)\delta^{(\mathrm{DB})}_{\kappa=-\ell-1} + \ell\delta^{(\mathrm{DB})}_{\kappa=\ell}\right] \tag{134a}$$

and

$$\mathcal{G}_\ell = \frac{1}{2\mathrm{i}k}\Big[\exp\left(2\mathrm{i}\delta_{\kappa=-\ell-1}\right) - \exp\left(2\mathrm{i}\delta_{\kappa=\ell}\right)\Big] - \frac{1}{k}\left[\delta^{(\mathrm{DB})}_{\kappa=-\ell-1} - \delta^{(\mathrm{DB})}_{\kappa=-\ell}\right]. \tag{134b}$$

For angles larger than about 1 degree, the convergence can be accelerated further by means of the reduced series method [31,32].

7. The program ECCPA

The Fortran program ECCPA calculates DCSs for elastic collisions of charged particles with atoms by using the theory and approximations presented in the previous Sections. The program delivers the DCSs obtained from the classical trajectory method (Section 3.2), the Born approximation (Section 4.2), the eikonal approximation (Section 4.4), and the partial-wave expansion method with Born and WKB phase shifts (Section 4.3). In the case of electrons and muons, the program can use the Born approximation and the partial-wave expansion method that result from the Dirac wave equation (Sections 6.1 and 6.2).

The program utilizes robust numerical methods. In particular, integrals of functions defined by an analytical formula are calculated by using the Fortran external function `sumga` [10], which implements an adaptive algorithm, based on the 20-point Gauss-Legendre quadrature formula and a bisection scheme, and allows a strict control of integration errors. Continuous functions that occur at intermediate steps of the calculation, are first tabulated at the points of a non-uniform grid of the variable, which is determined adaptively by placing more points in regions where the function varies more rapidly. Subsequently, function values are calculated by linear or logarithmic natural cubic spline interpolation [43,44]. Bessel functions of integer orders are calculated by using the Fortran double-precision subroutines of Takuya Ooura (http://www.kurims.kyoto-u.ac.jp/~ooura/).

The calculation of the classical DCS starts by setting a table of the deflection function $\vartheta'(L')$, Eq. (46), which is computed by means of function `sumga` to a relative accuracy of about $\sim 10^{-7}$ for a dense grid of angular momenta. This table extends to very small and very large angular momenta, from $\sim 10^{-7}\hbar$ to $\sim 10^{8}\hbar$, to ensure accuracy of the calculated DCS at small and large angles. When the `sumga` function cannot attain a required accuracy of at least three decimal places, the program issues a warning message. The program produces a table of the classical DCS, Eq. (51), and of the quantity $T_{\mathrm{class}}(\theta')$, Eq. (53), which allows verifying whether the classical calculation satisfies the Bohr validity criterion. At small angles, when the classical calculation does not comply with the validity criterion or when the DCS differs from the eikonal DCS by more than 10%, the classical DCS is set to zero.

The eikonal scattering amplitude is evaluated from the Zeitler and Olsen formula (95) by using the `sumga` function. The result is generally accurate to four or more digits for scattering angles less than the practical cutoff θ_{eik}, Eq. (98). For larger angles, the analytical extrapolation (99) is used. The WKB phase shifts, Eq. (81) and (130) are also calculated by means of the `sumga` function to a relative accuracy of about 10^{-10}. In the summation of partial-wave series, Eqs. (85) and (133), the reduced-series method is applied for scattering angles larger than 1 degree. For projectiles with very high energies, it may be impossible to achieve convergence of the partial-wave series at angles less than 1 degree because of the limited memory storage allowed and the accumulated round-off errors. In such case, the program replaces the partial-wave DCS with the eikonal approximation, which is generally accurate at small angles. When the kinetic energy of the projectile is too low for the eikonal approximation to be valid, the eikonal DCS is set to zero.

The user can select the projectile particle (the allowed options are electrons, positrons, muons, antimuons, protons, antiprotons, and alphas), the atomic number of the target atom (from $Z = 1$ to 99), and the parameterization of the atomic potential (see Section 2). To allow studying the effect of the relativistic terms of the effective potential, Eq. (38), classical trajectories and WKB phase shifts may be evaluated by using either of the following potentials:

1) the bare electrostatic potential $V(r)$,
2) the potential with the second-order correction given by Eq. (39a),

$$V(r) - \frac{V^2(r)}{2\mu_{\mathrm{r}}c^2}\left(1 - \frac{3\mu_{\mathrm{r}}c^2}{\mathcal{S}}\right), \tag{135}$$

   which reduces to the Klein-Gordon potential for a target atom with infinite mass, or
3) the full effective potential (38).

However, the Born DCS and phase shifts and the eikonal DCS are always calculated with only the electrostatic potential $V(r)$ because their calculation algorithms rest on the assumed analytical form of the potential [sum of Yukawa terms, Eq. (5)].

The program ECCPA generates a main output file, named `dcs.dat`, that contains a global description of the considered collision process and a table of calculated DCSs with the various theoretical approaches for a predefined grid of 1,000 scattering angles in CM. This file also includes the corresponding values of the total cross section, Eq. (100), the momentum transfer cross section, Eq. (101), and the second transport cross section,

$$\sigma_2 = \int \left[1 - P_2(\cos\theta')\right] \frac{\mathrm{d}\sigma'}{\mathrm{d}\Omega'}\,\mathrm{d}\Omega' = \int \frac{3}{2}(1-\cos^2\theta')\frac{\mathrm{d}\sigma'}{\mathrm{d}\Omega'}\,\mathrm{d}\Omega'. \tag{136}$$

Because the classical and partial-wave DCSs may present calculation artifacts in difficult cases, these integrals are calculated by linear log-log interpolation of the DCS tables, a method that is not highly accurate but is generally robust against numerical fluctuations. Additionally,

Table 2
Example of input data file for the ECCPA program. The scale lines are not part of the file.

```
C...+....1....+....2....+....3....+....4....+....5....+....6....+..
6         Projectile (1=e-, 2=e+, 3=mu-, 4=mu+, 5=p+, 6=p-, 7=alpha)
1         Wave equation (1=Schrod, 2=Schrod M=infty, 3=Dirac)
3         Potential (1=V(r), 2=+1st corr, 3=+1st+2nd corrs)
1         Screening model (1=DHFS, 2=TFM, 3=Wentzel)
80        Atomic number
1e8       Kinetic energy in LAB, as many lines as needed...
1e9
C...+....1....+....2....+....3....+....4....+....5....+....6....+..
```

the program produces several output files with results from intermediate stages of the calculation and with complementary information. The calculation of the set of DCSs for each specific case (*i.e.*, target atom, projectile type, and kinetic energy of the projectile in L) takes only a few seconds on an Intel i7 processor, quite independently of the details of the case.

The ECCPA program is devised to run interactively. The user may enter the parameters of the problem directly from the keyboard, in response to prompts from the program, which are self-explanatory. The distribution bundle includes scripts for visualizing the contents of output files by means of the plotting software GNUPLOT (http://www.gnuplot.info/). Alternatively the program can read data from an input file and be run in batch mode, allowing the calculation of cross sections for multiple energies of the projectile in a single run.

The input file provides the same information that would be entered from the keyboard. Each line in this file contains numerical values (in free format) followed by a brief text description (a reminder to the user, not read by the program). Table 2 shows an example of input file for antiprotons colliding with mercury atoms. The information in the file is the following:

- 1st line. Kind of projectile, an integer, with the possible values 1 (electron), 2 (positron), 3 (muon), 4 (antimuon), 5 (proton), 6 (antiproton), and 7 (alpha particle).
- 2nd line. Considered wave equation, identified by the integer parameter `IWEQ`

$$\begin{aligned} \texttt{IWEQ} = 1,&\ \text{Schrodinger equation},\\ = 2,&\ \text{Schrodinger equation with } M_2 = \infty,\\ = 3,&\ \text{Dirac equation with } M_2 = \infty \text{ (for electrons and muons only)}, \end{aligned}$$

- 3rd line. Potential type used in the calculations, defined by the integer parameter `IVEF`

$$\begin{aligned} \texttt{IVEF} = 1,&\ \text{the atomic potential, } V(r),\\ = 2,&\ \text{the sum } V(r) + V_{\rm r1}(r),\\ = 3,&\ \text{the full effective potential, } V_{\rm eff} = V(r) + V_{\rm r1}(r) + V_{\rm r2}(r). \end{aligned}$$

- 4th line. Screening function parameterization: 1 (DHFS), 2 (TFM), and 3 (Wentzel).
- 5th line. Atomic number Z (from 1 to 99) of the target atom.
- 6th and following lines. Kinetic energy of the projectile in the L frame, in eV. A single value in each line, as many lines as needed.

To facilitate the use of the program in interactive mode, the distribution bundle includes the Java graphical user interface (GUI) ECCPA.JAR, which runs under Microsoft Windows 10, Linux, and macOS operating systems. This GUI not only simplifies the writing of input data but also provides a plotting tool for visualizing the calculation results. The container window of the GUI consists of a menu with two tabs, a left control panel with a series of buttons and tabs, a pair of buttons to inspect the calculation report and to produce a screenshot in png format, a status bar, and a plotting area that is active only at the end of a calculation. The menu tab "select&compute" opens the input panel to display four buttons that allow defining the desired calculation (projectile kind, wave equation, potential model, and electronic screening model) through context menus, a button that opens a periodic table of the elements to select the target atom, a text tab to enter the kinetic energy of the projectile, and a button to run the ECCPA code with the selected options. When the calculation is completed, the "plot" menu tab is automatically activated and the left control panel allows selecting the results to be plotted. The details of a plot can be changed through context menus and windows that are opened with the right bottom of the mouse when the pointer is in specific areas. Fig. 1 shows the container window just before starting the calculation, with the input data entered in the left panel (the same as in Table 2) and the active periodic table. Fig. 2 shows the plot window of the GUI with the DCS obtained from that calculation.

8. Sample calculation results

To illustrate the reliability of the different calculation approaches, Figs. 3 and 4 display calculated DCSs for collisions of various projectiles with mercury atoms. For projectiles heavier than the electron, Fig. 3, the Born approximation is seen to fail for projectiles with low energies and at small angles. The classical calculation for antiprotons and alphas is valid for the whole angular range covered in the plots (although it fails at small angles), and it is in close agreement with the DCS computed by the partial-wave method with approximate phase shifts and by the eikonal approximation. Calculation results indicate that the eikonal approximation provides a reliable description of collisions with scattering angles less than about 30 degrees.

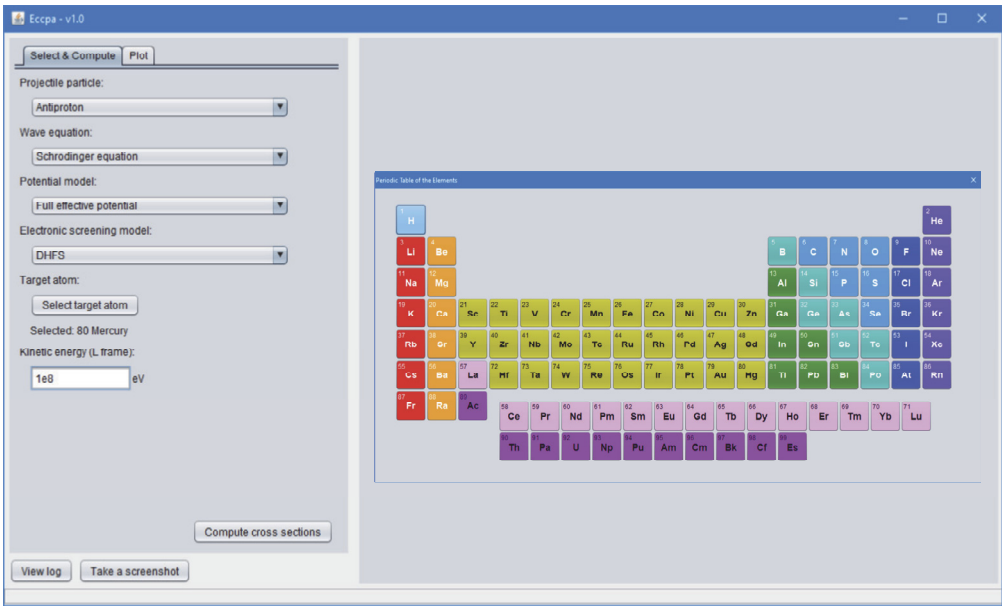

Fig. 1. Container window of the GUI, showing entered input data and the active periodic table.

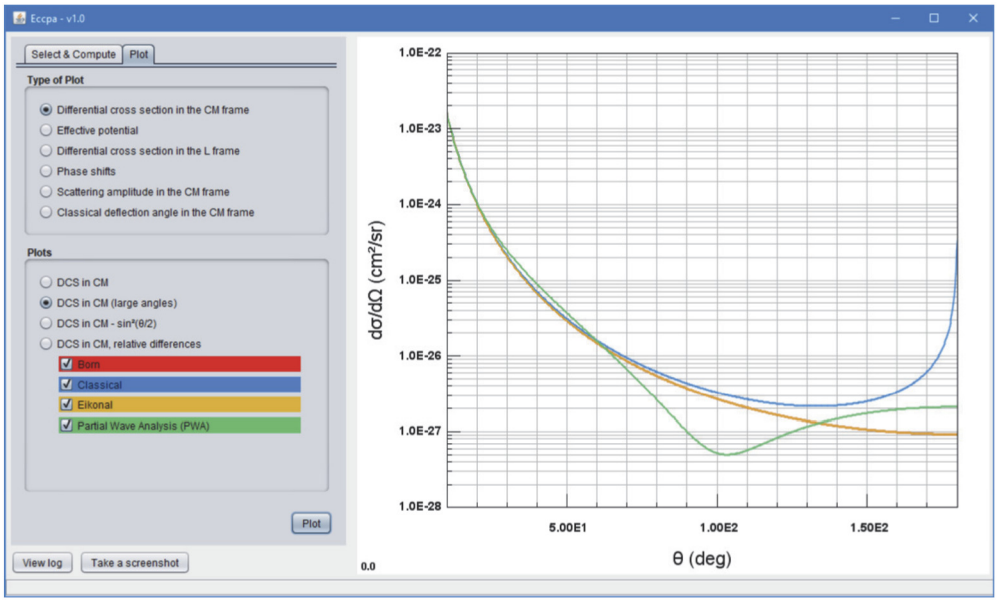

Fig. 2. Plot window of the GUI ECCPA.JAR, displaying the calculated DCS in CM for scattering angles larger than 10 degrees.

It is worth mentioning that the actual DCS for elastic collisions of protons and heavier charged particles with atoms is sensitive to the size and structure of the atomic nucleus, which determines the DCS at angles larger than about 10 degrees (see, *e.g.*, [25]). The total probability $P(\theta > 10°)$ of scattering angles larger than 10 degrees in a collision increases with the atomic number of the target atom. In the case of protons colliding with mercury atoms, $P(\theta > 10°)$ is about 10^{-6}, 10^{-8}, and 10^{-11}, for $E = 10$ MeV, 10^3 MeV, and 10^5 MeV, respectively. Consequently, in transport calculations of protons and heavier particles, it is generally justified to utilize DCSs calculated with only the electrostatic potential, disregarding both the relativistic correction terms and the size of the nucleus.

Results of ECCPA calculations for electrons and positrons using the Dirac equation with the DHFS potential are displayed in Fig. 4. For comparison purposes, the plots include the DCSs calculated numerically with the program ELECTRONSCAT of the RADIAL package [20] for the same potential. That program implements a partial-wave calculation with highly accurate phase-shifts, combined with the reduced-series method to accelerate the convergence of the partial-wave series for the scattering amplitudes. Results from our partial-wave calculation with approximate phase shifts are seen to agree closely with the numerical results calculated by ELECTRONSCAT except at large angles, reflecting the limitations of the WKB approximation for phase shifts with small $|\kappa|$ values. The close agreement between the eikonal and partial-wave results at small angles (up to ∼30 degrees) is noteworthy. For collisions of positrons and electrons, the eikonal approximation is better than acceptable, except for projectile energies less than about 10 keV.

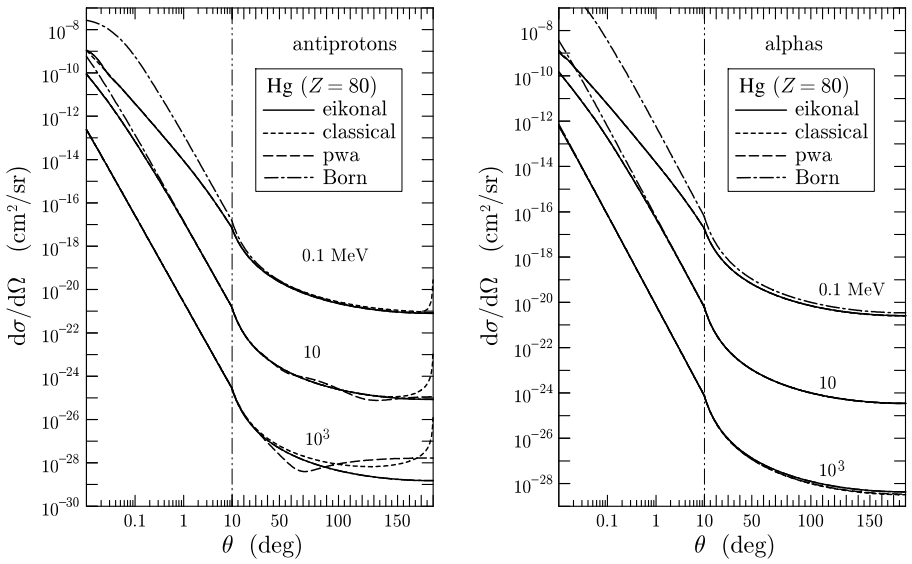

Fig. 3. DCSs (in CM) for collisions of antiprotons and alphas with mercury atoms, calculated for the DHFS potential by using the approximations indicated in the legend: eikonal approximation (solid curves), classical trajectory method (dotted), partial-wave analysis with approximate phase shifts (dashed) and Born approximation (dot-dashed). The labels indicate the kinetic energy of the projectile (in L). Notice the logarithmic scale for $\theta < 10°$.

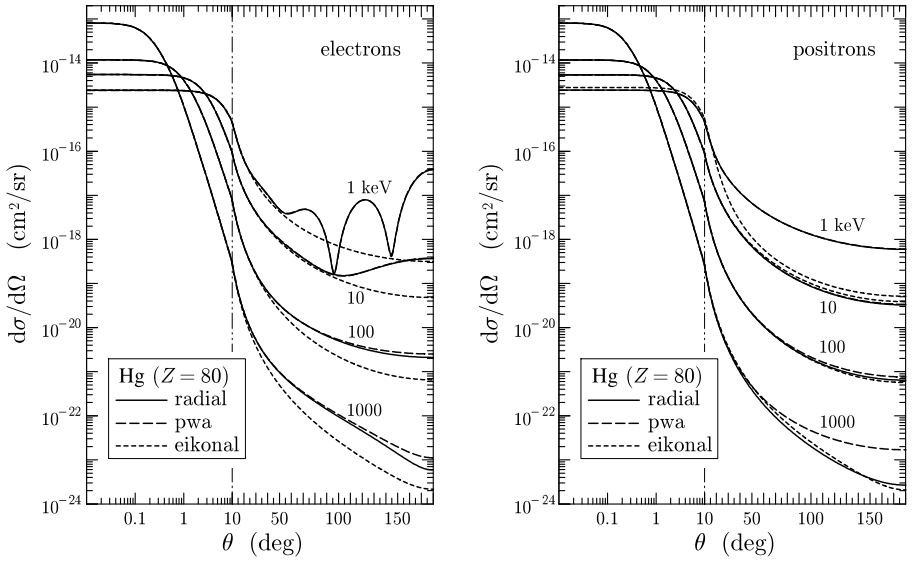

Fig. 4. Calculated DCS for elastic collisions of electrons and positrons with mercury atoms. Solid curves represent the results from the program ELECTRONSCAT [20]. The dashed curves represent DCSs calculated with the present partial-wave method with approximate (WKB and Born) phase shifts. The dotted curves are DCSs obtained from the eikonal approximation. Notice the logarithmic scale for $\theta < 10°$.

Declaration of competing interest

The authors declare that they have no known competing financial interests or personal relationships that could have appeared to influence the work reported in this paper.

Acknowledgements

Financial support from the Spanish Ministerio de Ciencia, Innovación y Universidades / Agencia Estatal de Investigación / European Regional Development Fund, European Union (projects no. RTI2018-098117-B-C22 and PID2019-104888GB-I00) and from Junta de Andalucía (projects no. FQM387 and P18-RT-3237) is gratefully acknowledged.

References

[1] L.D. Landau, E.M. Lifshitz, Mechanics, 2nd English edition, Pergamon Press, Oxford, 1969.
[2] H. Goldstein, Classical Mechanics, Addison-Wesley, Reading, MA, 1980.
[3] L.I. Schiff, Quantum Mechanics, McGraw-Hill, Tokyo, 1968.
[4] E. Merzbacher, Quantum Mechanics, 3rd edition, John Wiley and Sons, New York, 1970.
[5] J.J. Sakurai, Modern Quantum Mechanics, rev. edition, Addison and Wesley, New York, 1994.
[6] E. Rutherford, Philos. Mag. Ser. 6 21 (125) (1911) 669–688.

[7] C. O'Raifeartaigh, J.F. McGilp, Comput. Phys. Commun. 28 (1983) 255–264.
[8] F. Salvat, A. Jablonski, C.J. Powell, Comput. Phys. Commun. 165 (2005) 157–190.
[9] M.J. Berger, in: B. Alder, S. Fernbach, M. Rotenberg (Eds.), Methods in Computational Physics, vol. 1, Academic Press, New York, 1963, pp. 135–215.
[10] F. Salvat, PENELOPE-2018: A Code System for Monte Carlo Simulation of Electron and Photon Transport, Document NEA/MBDAV/R(2019)1, OECD Nuclear Energy Agency, Boulogne-Billancourt, France, 2019.
[11] N.F. Mott, H.S.W. Massey, The Theory of Atomic Collisions, Oxford University Press, London, 1965.
[12] C.J. Joachain, Quantum Collision Theory, North Holland, Amsterdam, 1975.
[13] F. Salvat, Phys. Rev. A 68 (2003) 012708.
[14] G. Molière, Z. Naturforsch. 3a (1948) 78–97.
[15] J.F. Ziegler, J.P. Biersack, M.D. Ziegler, SRIM the stopping and range of ions in matter, www.srim.org, www.lulu.com, 2012.
[16] V. Bush, S.H. Caldwell, Phys. Rev. 38 (1931) 1898–1902.
[17] G. Molière, Z. Naturforsch. 2a (1947) 133–145.
[18] F. Salvat, J.D. Martínez, R. Mayol, J. Parellada, Phys. Rev. A 36 (1987) 467–474.
[19] D. Liberman, D.T. Cromer, J.T. Waber, Comput. Phys. Commun. 2 (1971) 107–113.
[20] F. Salvat, J.M. Fernández-Varea, Comput. Phys. Commun. 240 (2019) 165–177, see also the manual of the computer code.
[21] G. Wentzel, Z. Phys. 42 (1927) 590–593.
[22] J.D. Jackson, Classical Electrodynamics, 2nd edition, John Wiley and Sons, New York, 1975.
[23] E. Everhart, G. Stone, R.J. Carbone, Phys. Rev. 99 (1955) 1287–1290.
[24] N. Bohr, K. Dan. Vidensk. Selsk. Mat. Fys. Medd. 18 (8) (1948) 1–144.
[25] F. Salvat, J.M. Quesada, Nucl. Instrum. Meth. B 475 (2020) 49–62.
[26] A. Messiah, Quantum Mechanics, Dover Publications Inc., New York, 1999.
[27] G. Baym, Lectures in Quantum Mechanics, Westview Press, Boulder, Colorado, 1974.
[28] I.S. Gradshteyn, I.M. Ryzhik, Table of Integrals, Series, and Products, 3rd edition, Elsevier - Academic Press, London, 2007.
[29] M. Abramowitz, I.A. Stegun, Handbook of Mathematical Functions, Dover, New York, 1972.
[30] J.M. Fernández-Varea, R. Mayol, J. Baró, F. Salvat, Nucl. Instrum. Meth. B 73 (1993) 447–473.
[31] D.R. Yennie, D.G. Ravenhall, R.N. Wilson, Phys. Rev. 95 (1954) 500–512.
[32] ICRU Report 77, Elastic Scattering of Electrons and Positrons, ICRU, Bethesda, MD, 2007.
[33] R.E. Langer, Phys. Rev. 51 (1937) 669–676.
[34] S.J. Wallace, Phys. Rev. Lett. 27 (1971) 622–625.
[35] F.W. Byron, C.J. Joachain, Phys. Rev. A 15 (1977) 128–146.
[36] E. Zeitler, H. Olsen, Phys. Rev. 136 (1964) A1546–A1552.
[37] F. Salvat, Nucl. Instrum. Meth. B 316 (2013) 144–159.
[38] E. Zeitler, H. Olsen, Phys. Rev. 162 (1967) 1439–1447.
[39] M.E. Rose, Relativistic Electron Theory, John Wiley and Sons, New York, 1961.
[40] D.W. Walker, Adv. Phys. 20 (1971) 257–323.
[41] G. Parzen, Phys. Rev. 80 (1950) 261–268.
[42] B.H. Bransden, C.J. Joachain, Physics of Atoms and Molecules, Longman, Essex, England, 1983.
[43] W.H. Press, S.A. Teukolski, W. Vetterling, B. Flannery, Numerical Recipes in Fortran 77. The Art of Scientific Computing, 2nd edition, Cambridge University Press, New York, 1992.
[44] P.L. DeVries, A First Course in Computational Physics, John Wiley and Sons, Inc., New York, 1994.